Development of a Poly(Methyl Methacrylate-*co*-*n*-Butyl Methacrylate) Copolymer Binder System

N. K. VAIL,[1,*] J. W. BARLOW,[1] J. J. BEAMAN,[2] H. L. MARCUS,[2] and D. L. BOURELL[2]

[1]The Department of Chemical Engineering, and [2]The Department of Mechanical Engineering, Center for Materials Science and Engineering, The University of Texas at Austin, Austin, Texas 78712

SYNOPSIS

Low molecular weight poly(methylmethacrylate) and poly(methylmethacrylate-*co*-*n*-butylmethacrylate) emulsion-based polymers are developed for use as fugitive binders of high temperature powders to be used with the rapid prototyping method known as selective laser sintering. Kinetics of the homopolymerization of methylmethacrylate and *n*-butylmethacrylate are found to deviate from Smith-Ewart Type II predictions. Reactivity ratios for the monomer pair are determined and indicate the pair to yield random copolymers. Molecular weight was controlled by the addition of chain transfer agents. Several transfer agents were studied and one, *iso*-octyl-3-mercaptopropionate, was selected for use with emulsion polymerizations. Glass transition temperatures of the homopolymers and copolymers were studied. © 1994 John Wiley & Sons, Inc.

INTRODUCTION

Several novel solid freeform fabrication[1,2] processes have emerged as rapid prototyping and manufacturing methods for preparing three dimensional objects. These processes differ radically from conventional fabrication methods in that they produce three dimensional objects by some means of material addition. One of these techniques, Selective Laser Sintering™, or SLS, was developed at The University of Texas in the late 1980s.[3,4] Selective Laser Sintering has been developed into a commercial process by DTM Corporation, Austin, Texas, and has become a leader in the field of rapid prototyping using fusible polymer powders, such as bisphenol-A polycarbonate, nylon 11, and investment casting waxes.

As shown in Figure 1, the SLS process consists of a laser with scanning control (A, B), a computer for process control (H), a powder leveling mechanism (D), a powder feed cylinder (not shown), a part cylinder (F), and a radiant heater for maintaining powder bed temperatures (C). Processing takes place in an inert, temperature-controlled atmosphere. Files for three-dimensional parts are typically generated with CAD systems that have solid modeling capabilities. These files are numerically sliced via additional software into layers. Each layer corresponds to a layer of powder. Powder layers are delivered by the leveling mechanism from the powder feed cylinder to the part cylinder. Layer thicknesses are selected by the operator to be in the range of 0.010 to 0.025 centimeters. The software layer information is used to drive the scanning laser. The laser selectively sinters the area corresponding to the current layer of the part. Enough energy is provided by the laser to fuse the powder within the layer and to fuse the current layer to any previous layers. In this manner, a three-dimensional object is built from the bottom up. No part supports are necessary, because the unsintered powder provides a natural support. The unsintered powder is easily brushed away, leaving the solid object.

The SLS manufacturing process can be adapted to form parts directly from high temperature fusible materials, such as ceramics and metals.[5] This process advancement is presently under development at The University of Texas at Austin. Research is also focused on the development of composite ceramic and metal powders that contain fugitive polymer binders.[6-8] The polymer binder is combined with the

* To whom correspondence should be addressed.

Journal of Applied Polymer Science, Vol. 52, 789–812 (1994)
 CCC 0021-8995/94/060789-24

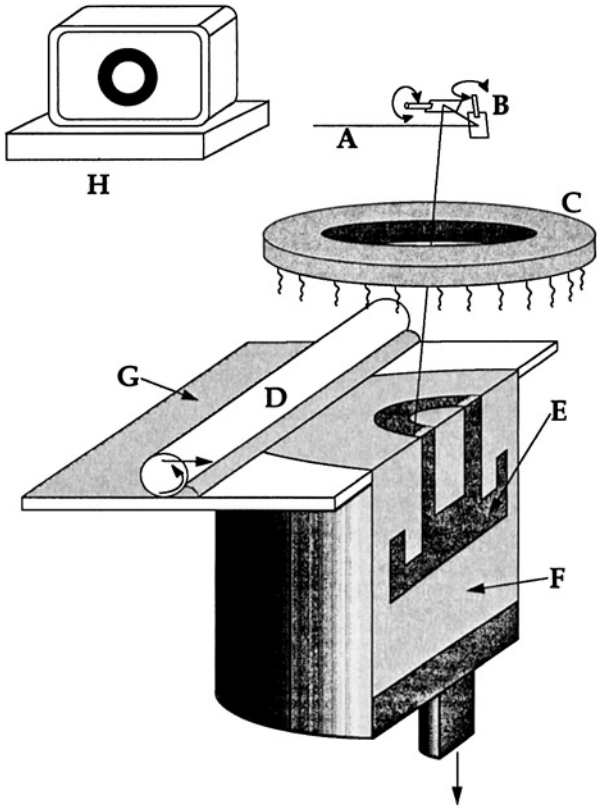

Figure 1 Selective laser sintering process. (A) Laser source, (B) mirrors, (C) radiant heater, (D) leveling mechanism, (E) part, (F) powder bed, (G) new layer, and (H) computer control.

high temperature powder material and the resulting composite is subjected to conventional SLS processing. This yields a polymer-bound object, normally termed a "green" part, that can be postprocessed to yield a functional part.

Preliminary investigations have shown that encapsulation of the inorganic powders with the polymer binder offers distinct advantages over simply mixing the binder with powders.[9] Encapsulated powders do not suffer from segregation caused by density differences of the constituents, whereas powder mixtures of low density binder with high density materials clearly show separation with only slight tapping. In addition, for a given volume fraction of binder, green parts, made from polymer encapsulated powders, exhibit green strengths that are greater than those of green parts made from mixed powders. In other words, a lower polymer content is required in encapsulated powders than in mixed powders to obtain a given green strength. This requirement is essential to obtaining green parts with high ceramic or metal contents. Also, most of the ceramic and metal powders under consideration have particle sizes in the range of 0.1–10 μm. Powders of this size range often spread poorly during the SLS leveling sequence, resulting in low bed densities and discontinuous bed surfaces. Encapsulation with polymer binder can agglomerate these small particles to achieve composite particles with sizes in the range of 20–100 μm. Powder leveling is much improved when these larger particles are used.[10]

Spray drying[11] is the method of choice for encapsulation of ceramic and metal powders. This method offers the distinct advantage of yielding a free-flowing powder in a single step process. Many examples of encapsulation by spray drying can be found in the literature.[12] The method typically requires the encapsulating material be soluble in a carrier media that is easily vaporized. Several volatile organic solvents are potentially suitable for this purpose, however, these are not being considered, due to increased handling and processing requirements. This leaves polymers that are soluble or dispersible in water. Water soluble polymers have some technical drawbacks and are not being used in the present application. First, these polymers are sensitive to humidity and they can become rubbery or sticky if the humidity is too high, resulting in encapsulated particles that do not spread well with the SLS leveling mechanism. Second, most do not thermally degrade to only gaseous products under the reducing conditions required for processing metal parts. This characteristic can lead to carbon residue in the part following binder burnout and it can also lead to poor mechanical properties.

To avoid the problems discussed above, water-based emulsion polymer and copolymer binders were chosen to prepare coated inorganic powders for use in the SLS process. One of the binder systems chosen for this study, the preparation of which is discussed in detail in this article, is the emulsion copolymer comprising methylmethacrylate, MMA, and *n*-butylmethacrylate, *n*BMA. This system has several advantages. The first advantage is the ease of preparation of this essentially random copolymer by well-known free radical mechanisms.[13–17] Second, the copolymer has alternating 1,1-disubstituted carbons in its backbone. This feature permits depolymerization to monomer gases, resulting in low carbon residue during thermal removal of the binder,[18,19] even under the reducing conditions required for sintering of metals. The glass transition temperature, T_g, of the copolymer can be varied between 20°C, the T_g of pure P*n*BMA, and 110°C, the T_g for pure PMMA, by adjusting the copolymer composition.[20] Due to drying temperature limits on

our spray drier, binders with T_gs in excess of 110°C will not produce agglomerated and coated particles, therefore it is operationally useful to reduce the binder T_g to below 100°C. Powder storage and SLS roller-spreading concerns generally require that the T_g of the binder be no lower than 40–50°C. Some attraction and potential adhesion of PMMA to polar inorganic surfaces is indicated in the literature.[21-23] Adhesion is clearly important to the development of good green strengths, and this will be discussed in a subsequent article.

Regardless of the polymer or copolymer binder composition chosen, green strength, powder bed density, and agglomerate morphology are found to be related to the binder's ability to wet rapidly the inorganic particulate during spray drying. Toward that end, we deliberately produced low molecular weight (typically M_n = 10–25,000), high melt flow materials [melt flow near 30 g/10 min at 200°C and 0.52 MPa (75 psi) (ASTM D1238)]. As discussed below, this is accomplished in a batch mode by control of the polymerization recipe and by the use of chain transfer agents.

MATERIALS AND METHODS

Materials

Methylmethacrylate (MMA) and *n*-butylmethacrylate (*n*BMA) (Aldrich Chemical Co.) monomers were purified of inhibitor by washing three times with 5M NaOH solution at a volume ratio of 5 : 1, monomer to caustic, respectively. Washed monomers were chilled to −4°C to freeze residual water, were filtered, and were then stored at 4°C until needed. Clean monomers were used within two weeks of purification. Monomers, cleaned in this fashion, yielded repeatable results with little or no induction periods prior to initiation of polymerization.

Potassium persulfate initiator (Aldrich Chemical Co.) and electrophoresis grade sodium dodecyl sulfate (SDS) emulsifier (Kodak Chemical Co.), were used as supplied. Chain transfer agents thiophenol (THP) and *t*-dodecylmercaptan (*t*-DDM) were obtained from Aldrich Chemical Co. Additional chain transfer agents, *iso*-octyl-3-mercaptopropionate (*i*-OMP) and *n*-butyl-3-mercaptopropionate (*n*-BMP), were obtained from Pfaltz and Bauer Chemical Co. All chain transfer agents were used as received.

Table I Emulsion Polymerization Recipe

Ingredient	Quantity (g)
Deionized Water	100.00
Monomer	50.00
Potassium Persulfate	0.05–2.50
Sodium Dodecyl Sulfate	0.25–2.50

Preparation of Emulsion Polymers

Batch emulsion polymerizations were conducted using the general recipe presented in Table I. Filtered and deoxygenated water was used in all polymerizations. The reaction vessel consisted of a 500-ml, 3-necked, round-bottom flask, equipped with a 2 in. half-moon stirrer, connected to a stainless steel shaft, attached to a variable speed motor, a condenser, nitrogen and thermocouple inlets, and a glass sampling tube. The reaction vessel was immersed in a constant temperature water bath, equipped with an agitator, water inlet, and a temperature controller, capable of maintaining ±0.5°C.

Emulsifier and 75% of the total volume of water were added to the reaction vessel, were stirred, and were sparged with oxygen-free nitrogen for at least 15 min. Monomer, agitated and sparged with nitrogen for $\frac{1}{4}$ h prior to use, was then added to the reaction vessel. The vessel contents were emulsified for 15 min under a slightly positive pressure of nitrogen. During this period, the initiator was dissolved in the remaining portion of oxygen-free water and was brought to temperature by immersion in the water bath. The initiator solution was then added to the emulsion and the polymerization was carried out for a time sufficient to ensure complete conversion, typically no more than 6 h.

When chain transfer agents were used, the desired chain transfer agent (CTA) was added to the monomer and the resulting solution was charged to the reaction vessel. For the determination of the chain transfer constant, C_s, of a particular CTA/monomer system, the CTA was added to the monomer in the amounts of 0.1, 0.2, 0.4, and 0.8% (mol/mol).

Monomer conversion was determined gravimetrically. A total of 24 samples, 1–2 mL in volume, were withdrawn from the reaction vessel via the glass sampling tube at predetermined intervals. Each sample was drawn into a preweighed vial containing a 1% solution of hydroquinone (Aldrich Chemical Co.) in water to stop the reaction, was quickly weighed, and was then transferred to a preweighed aluminum pan. The samples were dried in a hood at room temperature. The samples were transferred to a vacuum oven and were maintained at 80°C for

6 h, were cooled, and were weighed. This process was repeated until constant weight was obtained.

Latex and Polymer Characterizations

The resulting latexes were filtered through glass wool to remove any coagulum. A portion of each latex was precipitated with acetone, was rinsed several times with deionized water, and was filtered. The resulting cake was spread on an aluminum sheet and was dried in vacuum.

Further portions of each latex were diluted with freshly distilled water to 0.0075% solids for viewing by scanning transmission electron microscopy (STEM). A monodisperse polystyrene standard latex (D_p = 1.40 ± 0.03 μm, Polysciences, Inc.) was added to the latex samples for internal calibration. The diluted samples were mounted on copper stages, which had been polished with 6 μm diamond paste (Buehler), followed by fine polishing with 0.05 μm alumina. The mounted samples were gold coated and photographed with a JEOL 1200× STEM, using an accelerating voltage of 120 keV. The resulting micrographs were digitally scanned to a high resolution image file that was processed manually for particle size information using a public domain image processing software package called Image, V1.41, published by the National Institutes of Health, available for MacIntosh computers.

Polymer molecular weights were determined by gel permeation chromatography (GPC), according to the method described by ASTM D3536-76, using a Waters liquid chromatograph, equipped with 10^5 Å, 10^4 Å, 10^3 Å, and 500 Å Ultrastyragel columns. The unit was further equipped with a Model R401 differential refractometer for detection. Chromatography was performed with tetrahydrofuran (HPCL Grade, Aldrich Chem. Co.) as the solvent. The columns were calibrated with narrow ($M_w/M_n \approx 1.0$) molecular weight polymethylmethacrylate standards (Pressure Chem. Co.), which had predetermined weight average molecular weights ranging from 6000 to 10^6.

Polymer melt flow, ASTM D1238, was determined using a Kayness Galaxy I capillary rheometer. Melt flow was determined at 200°C and 0.52 MPa (75 psi) for both PMMA and P(MMA-*co*-*n*BMA) polymers. Several measurements were done to obtain a representative average of the melt flow value.

Copolymer compositions were determined by nuclear magnetic resonance (NMR) spectroscopy. The 250-MHz ^{1}H spectra of polymers were recorded and analyzed on a Bruker AC-250 spectrometer, using 5% solutions in d_1-chloroform with tetramethylsilane (TMS) as an internal reference. Spectra were recorded at ambient temperatures.

Polymer glass transition temperatures, T_g, were measured using the differential scanning calorimetry (DSC) portion of a Perkin-Elmer Series 7 Thermal Analyzer System. Data were recorded at scanning rates of 10°C/min against a baseline scan. Temperature ranges of the scans were sufficient to allow at least 20°C prior to and following the transition of all polymers. For polymers having T_gs below about 40°C, it was necessary to modify the temperature ramp to scan at a rate of 5°C/min to provide more sensitivity.

RESULTS AND DISCUSSION

Determination of the Recipe

It was necessary to develop an emulsion recipe that could produce stable emulsions and yield measurable reaction rates at various temperatures for determination of kinetic information. Also, since minimal residue after thermal degradation is required, the recipe needed to use the minimum number of ingredients to obtain a low molecular weight polymer. Table I shows the general recipe that meets these criteria.

According to Type II Smith-Ewart emulsion homopolymerization kinetics with persulfate initiation,[24] the polymerization rate, R_p, and degree of polymerization, $\overline{DP}$, are related to initiator and emulsifier concentrations as follows

$$R_p \propto C_E^{0.6} C_I^{0.4}$$
$$\overline{DP} \propto C_E^{0.6} C_I^{-0.6} \quad (1)$$

where C_E is emulsifier concentration and C_I is initiator concentration. To verify this behavior, a series of experiments were conducted to determine the influence of C_E and C_I on polymerization rate, latex stability, and resultant polymer molecular weight. In these experiments, all maintained at 70°C ± 0.5°C, the initiator was varied over a hundredfold range and the emulsifier was varied over a tenfold range.

Figures 2 and 3 show the effect of C_E and C_I on the molecular weights of MMA and *n*BMA, respectively. The data confirm the general trends in molecular weight dependence described by Eq. (1), but give rise to different values for the exponents. The experimental exponents, associated with C_E and C_I, are determined to be 0.45 ± 0.06 and −0.52 ± 0.02 for MMA and 0.28 ± 0.04 and −0.35 ± 0.08 for

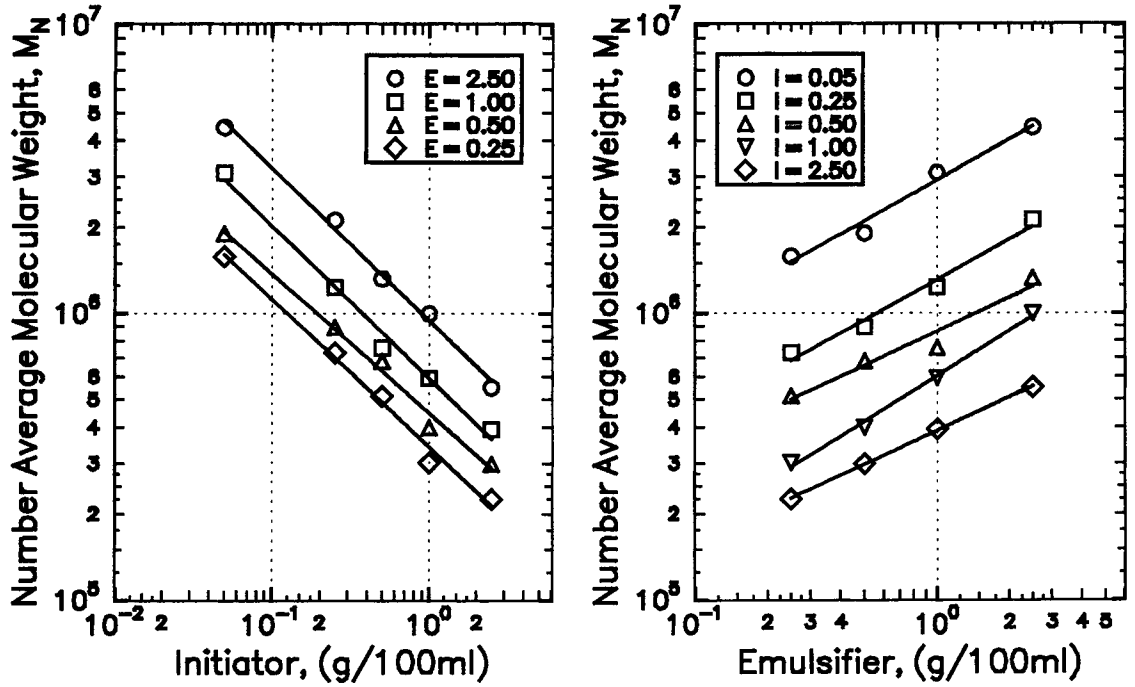

Figure 2 The effect of initiator and emulsifier concentrations on the molecular weight of emulsion polymerized methylmethacrylate, polymerized at 70°C.

*n*BMA, respectively. These values are presented without argument, since the intent was simply to observe the influences of emulsifier and initiator on molecular weight. Clearly, the combination of low emulsifier and high initiator concentrations yields the lowest molecular weight. However, the effect on

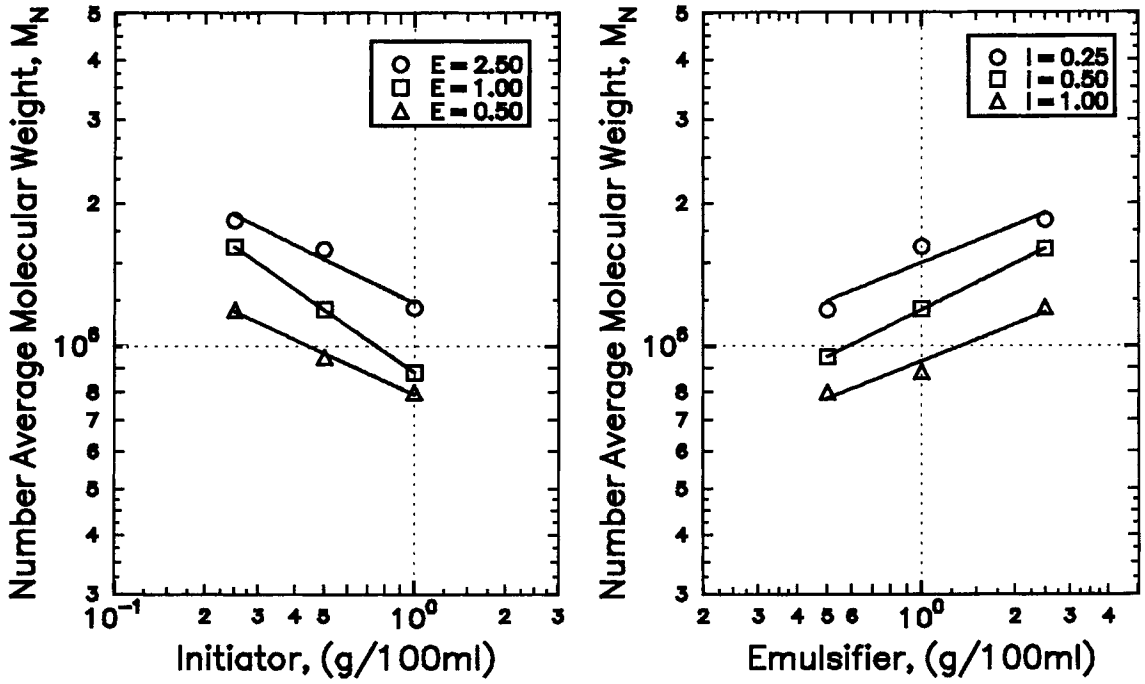

Figure 3 The effect of initiator and emulsifier concentrations on the molecular weight of emulsion polymerized *n*-butylmethacrylate, polymerized at 70°C.

Table II Summary of PMMA Latex Appearances for Various Initiator and Surfactant Concentrations

C_E (g/100 mL H_2O)	C_I (g/100 mL H_2O)	Temperature (°C)	Result
2.5	2.5	70	Stable
2.5	1.0	70	Stable
2.5	0.05	70	Stable
1.0	0.05	70	Stable
1.0	1.0	70	Stable
1.0	2.5	70	Cream
0.5	0.05	70	Stable
0.5	1.0	70	Clumps
0.5	2.5	70	Creamed
0.25	2.5	70	Solid
1.0	2.5	50	Cream
1.0	1.0	50	Stable
1.0	0.5	50	Stable

molecular weight is not especially pronounced. Both monomers show only about an order of magnitude change in M_n over the ranges of C_E and C_I studied. The molecular weights of all of these polymers are high, and the PMMA polymers show melt flows near zero at 200°C and 0.52 MPa (75 psi). Therefore, any appreciable changes in molecular weight can only be obtained by the addition of chain transfer agents.

At 70°C, polymerization rates for MMA were fast and difficult to measure accurately. The rate behavior, described by eq. (1), was qualitatively observed, but no rigorous analysis was conducted to determine the actual influences of C_E and C_I. The Trommsdorf or "gel effect" was observed in all polymerizations of MMA and was characterized by a substantial increase in the polymerization rate, R_p, accompanied by a 15–20°C increase in the reaction temperature. Consequently, isothermal conditions were difficult to maintain. Decreasing the emulsifier concentration reduced the rate as well as the exotherm caused by the gel effect. However, latex stability also decreased and the lower limit of stability was found to be approximately 0.5 g/100 mL, based on water, which is slightly more than twice the critical micelle concentration (8.1 mmol/L[25]) for SDS. At moderate to low concentrations of emulsifier, increases in the initiator concentration reduced latex stability. Table II summarizes PMMA latex stability observations.

The polymerization temperature was dropped to 50°C to reduce the exotherm. Emulsifier and initiator concentrations were fixed at 1 g/100 mL and 0.5 g/100 mL, based on water, respectively. Higher concentrations of initiator to favor low molecular weight were still found to reduce latex stability. The given concentrations yield latexes that have a minimum of ingredients, good emulsion stability, and nearly isothermal polymerization rates. The gel effect during polymerizations of MMA was reduced and reaction temperature increases did not exceed 5°C of the bath temperature.

Rate Kinetics

Using the recipe immediately above, the kinetics of homopolymerization of the monomers were determined in the temperature range of 30–60°C. Figure 4 shows representative conversion curves determined gravimetrically for homopolymerizations. The overall rate of polymerization, R_p, was determined from the slope of the constant rate period of the conversion curves. This region, termed Interval II, corresponds to an essentially constant polymer particle population, which is in thermodynamic equilibrium with dispersed monomer droplets. This results in a constant monomer concentration, $[M]$, within the growing polymer particles.[26]

Table III shows the results of particle size measurements for several PMMA emulsions. No particle size information for P*n*BMA latexes was obtained, due to the melting of these particles by the scanning electron beam. However, in the limited time before complete deformation of these latex particles, the apparent sizes were observed to be of the same order as the sizes observed for PMMA latexes. With respect to the PMMA latex particles, the high T_g of this polymer, combined with a sufficient gold coating, are sufficient to minimize deformation of the particles.[27]

Particle size distributions for the latexes shown in Table III were normally distributed with standard deviations, typically of about ±12 nm. Particle diameters, D_p, are expressed as a number average,[28] defined as

$$D_p = \frac{\sum n_i D_{p_i}}{\sum n_i} \tag{2}$$

where n_i is the number fraction of particles with diameter, D_{pi}, determined from microscopy. The number of polymer particles per milliliter, N, can then be determined according to the following[29]

$$N = \frac{6m_p}{\pi \rho_p D_p^3} \tag{3}$$

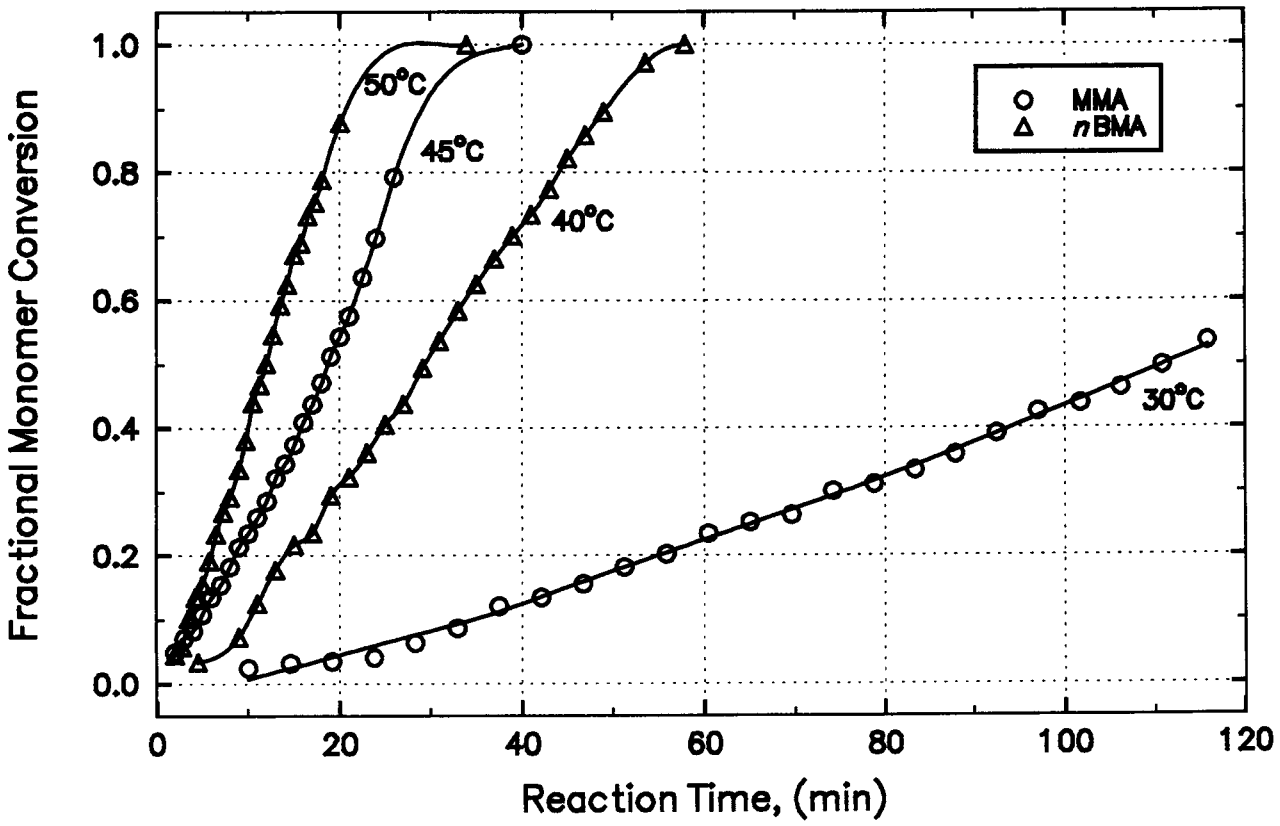

Figure 4 Typical monomer conversion curves for MMA (○) and *n*BMA (△), polymerized at various temperatures. C_I = 0.5 g/100 mL and C_E = 1.0 g/100 mL, based on water.

where m_p is the weight of polymer per milliliter of emulsion, ρ_p is the polymer density, and D_p is the particle diameter, determined from eq. (2). Assuming an emulsion density of approximately 1.0 g/cm^3, the weight of polymer per milliliter of emulsion, m_p, can be expressed as the mass fraction of polymer in the emulsion, x_p. This assumption yields values that are valid to within 7%. The density of PMMA is taken to be 1.188 g/cm^3 from the literature.[46]

Table III Particle Analysis for Emulsion Polymerization of MMA[a]

Run	Temperature (°C)	Solids (wt %)	Particle Diameter (nm)	N ($\times 10^{14}$/cm^3)
118	30	23.8	129	1.782
119	30	22.4	128	1.717
121	40	28.2	119	2.690
122	45	31.2	112	3.569
150	50	30.2	105	4.195
184	50	45.0	97	7.920
PP-2	50	44.6	126	3.584
PP-3	50	46.0	116	4.737
PP-4	50	44.7	109	5.549

[a] C_E = 1.0 g/100 mL and C_I = 0.5 g/100 mL, based on water.

The data of Table III show particle size to increase slightly with decreasing polymerization temperatures, therefore, there is a slight decrease in particle number with decreasing polymerization temperatures. This is consistent with other observations.[32] Generally, however, the number of particles appears to be fairly constant at about 2–5 $\times$ 10^{14} per milliliter. Therefore, in further considerations, a mean value of 4.0 $\times$ 10^{14} particles per milliliter is assumed.

Figures 5 and 6 show the Arrhenius plots of observed rates for MMA and *n*BMA, respectively. The activation energies are 21.78 kcal/mol and 17.91 kcal/mol, respectively. If Case II Smith–Ewart kinetics is observed, the polymerization rate can then be expressed as

$$-\frac{dm}{dt} = R_p = \bar{n} k_p [M] \frac{N}{N_A} \qquad (4)$$

where m is the monomer concentration of the emulsion, $\bar{n}$ is the number of radicals per polymer particle,

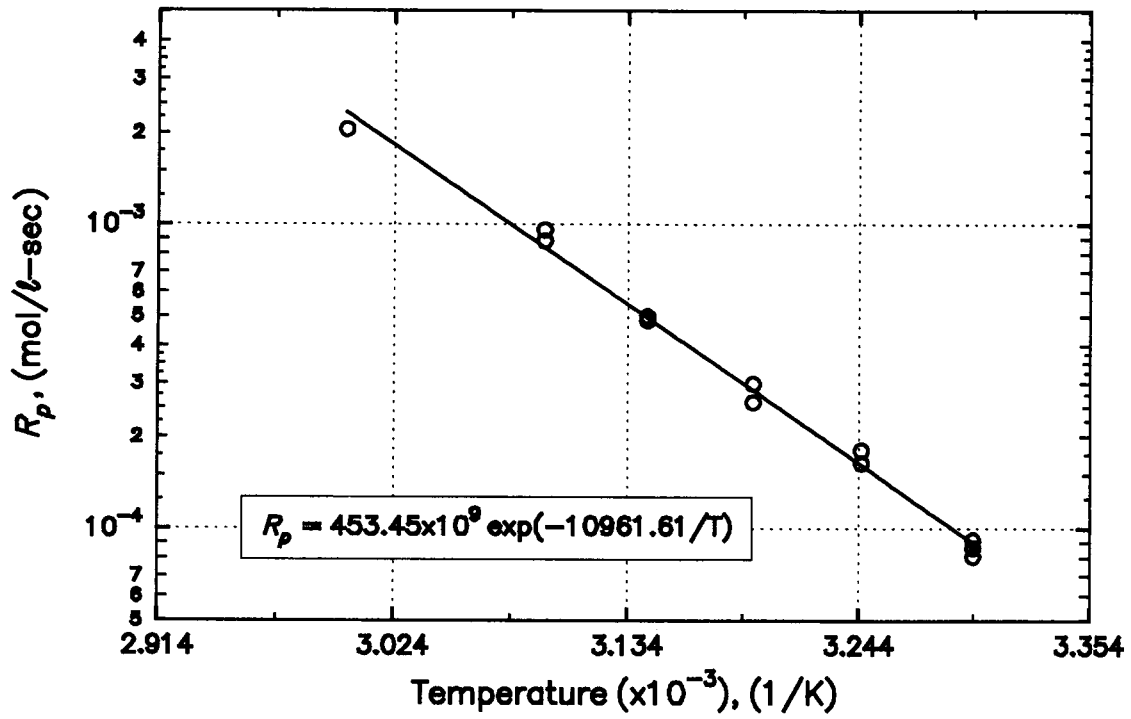

Figure 5 Effect of temperature on the emulsion polymerization rate of methylmethacrylate. C_I = 0.5 g/100 mL and C_E = 1.0 g/100 mL, based on water.

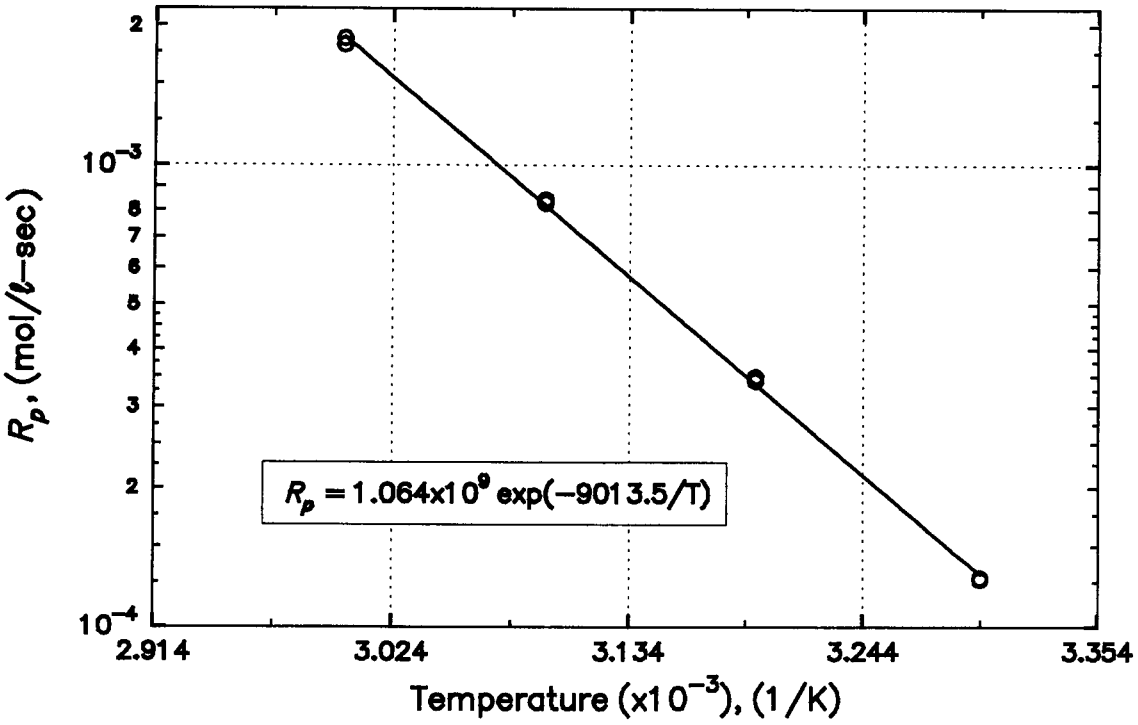

Figure 6 Effect of temperature on the emulsion polymerization of *n*-butylmethacrylate. C_I = 0.5 g/100 mL and C_E = 1.0 g/100 mL, based on water.

k_p is the propagation constant from homogeneous kinetics, $[M]$ is the monomer concentration in the polymer particles, N is the number particles per milliliter, and N_A is Avogadros' number. In the present work, the number of particles, N, has been shown to be essentially independent of temperature for PMMA. Similarly, monomer concentration in the polymer particles, $[M]$, is observed to be constant over a wide range of conditions.[26,30-32] Ballard et al.[31] used a value of 6.6 mol/L for PMMA latexes in their work. Gardon[26] determined a value of 4.5 $\pm$ 0.1 mol/L for P*n*BMA latexes. Assuming Case II Smith–Ewart kinetics, it follows that the determined activation energies should be those for the respective propagation constants. Typically, propagation constant activation energies for MMA range from about 4.4 kcal/mol[33] to about 7.5 kcal/mol.[46] Lora et al.[15] report propagation constant activation energies for MMA and *n*BMA as 5.45 kcal/mol and 4.87 kcal/mol, respectively, which is about a factor of four less than the determined values. Clearly, the observed rates deviate from Smith–Ewart kinetics and it is reasonable to conclude that $\bar{n}$ is not constant for the polymerizations. Brodnyan et al.[17] reported similar deviations of $\bar{n}$ for the monomers studied here and determined values of $\bar{n} \ll 0.5$, using the Stockmeyer analysis of Smith–Ewart kinetics. In the present study, using values of k_p for MMA determined by Lora et al.,[15] $\bar{n}$ is found to exist in a range from 0.3 at 30°C to 0.7 at 50°C.

At 50°C, the rates of polymerization, R_p, are 8.4 $\times 10^{-4}$ mol/L-s and 8.2 $\times 10^{-4}$ mol/L-s for MMA and *n*BMA, respectively. During copolymerization of MMA/*n*BMA, the measured rates did not differ significantly from the rates of the homopolymers. *n*BMA feed compositions, as little as 10% mole, were observed to eliminate the "gel effect" of MMA. This is probably due to decreases in polymer viscosity because of the presence of *n*BMA.

Reactivity Ratio Determination

Emulsion copolymerizations of MMA/*n*BMA were conducted over the entire range of monomer feed compositions, according to the plan outlined in Table IV. Copolymer compositions were determined by ^{1}H–NMR spectroscopy, from which a representative spectrum trace is shown in Figure 7. MMA monomer has a singlet peak at approximately δ = 3.8 ppm, corresponding to the methoxy of the ester linkage. Similarly, *n*BMA monomer shows a triplet peak at approximately δ = 4.2 ppm, corresponding to the ethyleneoxy of the ester linkage.[34,35] These two distinguishing peaks are easily identified in the spectrum shown in Figure 7 and for all other spectra for the copolymers studied. The respective monomer compositions of the copolymers were determined from the integrated peak areas, according to the following equation,

$$y_m = \frac{\frac{2h_m}{3h_b}}{1 + \frac{2h_m}{3h_b}} \tag{5}$$

where y_m is the mole fraction of methylmethacrylate in the copolymer, h_m is the methoxy peak area, h_b is the ethyleneoxy peak area, and the factor $\frac{2}{3}$ arises from the ratio of protons of the specific identifying groups.

The reactivity ratios of the monomers were determined from the polymer NMR composition data, according to the method of Fineman and Ross,[36] as modified by Kelen and Tüdős.[37] In the limit of low conversion, copolymer composition is described by the well known copolymer equation[38] as

$$\frac{m_1}{m_2} = \left(\frac{M_1}{M_2}\right)\left(\frac{r_1 M_1 + M_2}{r_2 M_2 + M_1}\right) \tag{6}$$

where m_1 and m_2 are concentrations of monomers in the copolymer, M_1 and M_2 are the concentrations of monomers MMA and *n*BMA, respectively, in the feed, and $r_1 = k_{11}/k_{12}$ and $r_2 = k_{22}/k_{21}$ are the monomer reactivity ratios for MMA and *n*BMA, respec-

Table IV Batch Copolymerization Monomer Feed Conditions

Latex No	MMA/*n*BMA Mole Ratio	MMA/*n*BMA Mass Ratio	Total Moles per 100 mL water
135, 151	95/5	13.38	0.49
136, 152	90/10	6.34	0.48
137, 153	85/15	3.99	0.47
138, 154	80/20	2.82	0.46
139, 156	75/25	2.11	0.45
140, 158	70/30	1.64	0.44
141, 160	65/35	1.31	0.43
142, 161	60/40	1.06	0.43
143, 163	55/45	0.86	0.42
144, 164	50/50	0.70	0.41
145, 165	40/60	0.47	0.40
148, 166	30/70	0.30	0.38
147, 167	20/80	0.18	0.37
149, 168	10/90	0.08	0.36

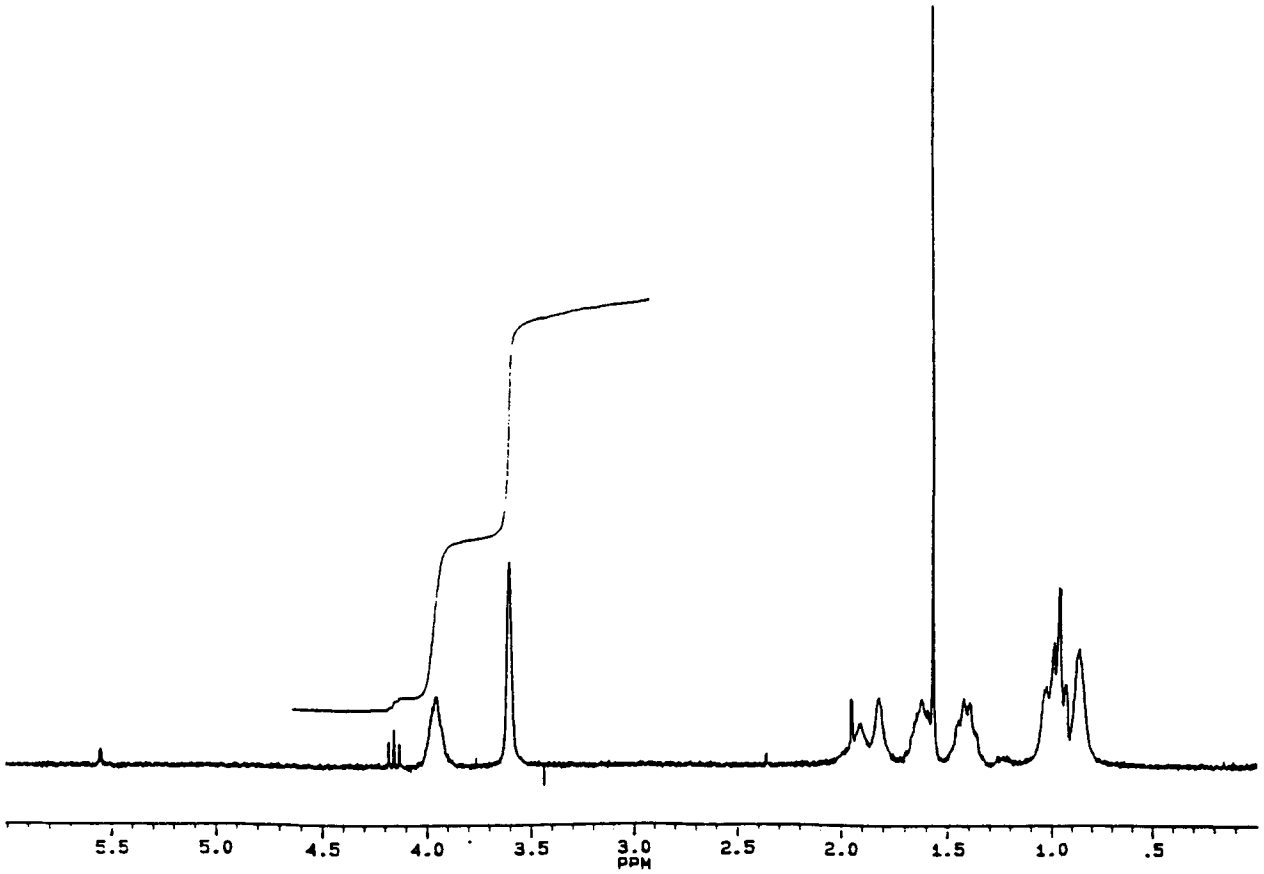

Figure 7 NMR spectrum trace for MMA/*n*BMA solution copolymer, polymerized at 70°C. Monomer molar feed ratio was 60/40 (MMA/*n*BMA).

tively. According to Fineman and Ross,[36] eq. (6) can be linearized into either of the forms

$$G = r_1 F - r_2$$

$$\frac{G}{F} = -r_2 \frac{1}{F} + r_1 \tag{7}$$

where $G = x(y-1)/y$, $F = x^2/y$, $x = M_1/M_2$, and $y = m_1/m_2$. Kelen and Tüdõs point out that eqs. (7) unequally emphasize data over the entire monomer feed composition range. Specifically, data obtained at the extreme monomer feed compositions greatly influence the least-squares regression and, therefore, influence the values of r_1 and r_2 obtained. To reduce the monomer feed extrema influence on the regression, they introduced a data dependent arbitrary constant, α, and redefined eqs. (7) as follows

$$\eta = \left(r_1 + \frac{r_2}{\alpha}\right)\xi - \frac{r_2}{\alpha} \tag{8}$$

where $\eta = G/(\alpha + F)$, $\xi = F/(\alpha + F)$, G and F are defined as above. Given an appropriate choice of α, the resultant values of ξ are evenly distributed over the interval (0, 1), much in the manner of the actual monomer feed mass fraction compositions. Usually $\alpha = 1$ is satisfactory, provided that $r_1 \approx r_2$. However, an improvement is to choose

$$\alpha = \sqrt{F_{\min} F_{\max}} \tag{9}$$

where $F_{\max}$ and $F_{\min}$ are the extrema of the parameter F, as defined previously.

Figure 8 shows the result of eq. (8) fitted to the experimental data. The parameter, α, determined for the data, had a value of 1.577, indicating the resultant reactivities would not be identical and $r_1 < r_2$. The values of r_1 and r_2, determined from the least-squares regression, were 0.758 ± 0.029 and 0.846 ± 0.044, respectively. As shown by Figure 9, these reactivities result in a slight deviation from ideality. Since $r_1 < r_2 < 1$, resulting copolymers tend to be random in nature and are slightly richer in

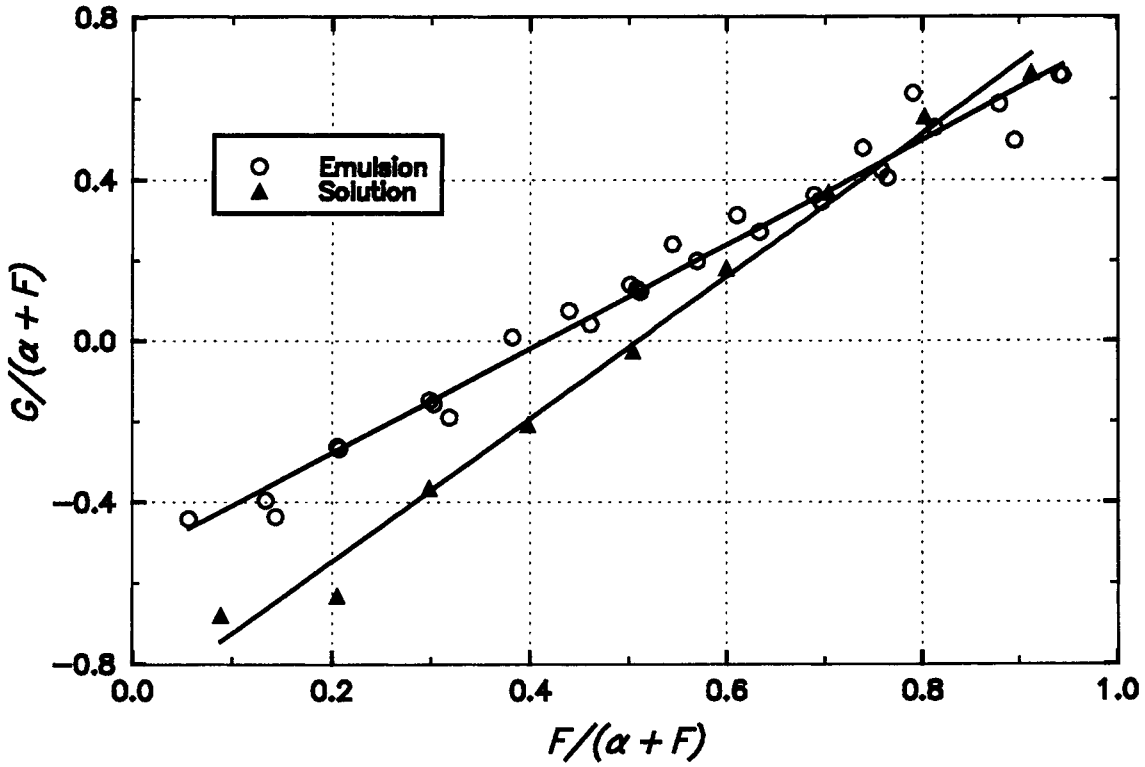

Figure 8 Kelen and Tüdõs[37] representation of MMA/*n*BMA composition data for copolymers polymerized in emulsion (○), α = 1.577, and polymerized in solution (▲), α = 1.034.

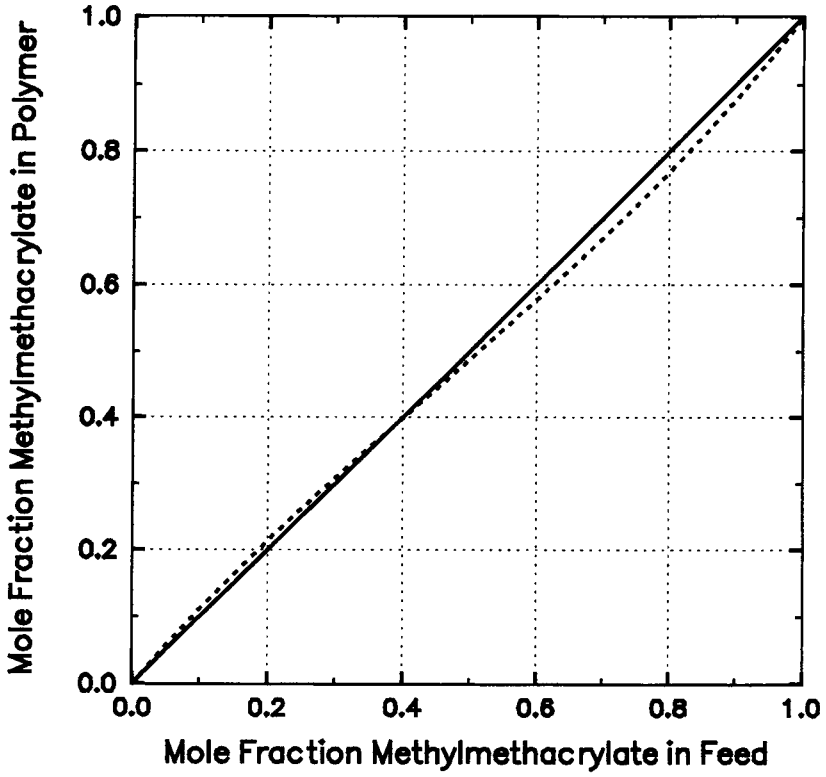

Figure 9 Instantaneous composition of emulsion copolymer as a function of monomer feed composition. (– – –) Copolymer and (——) ideal random copolymer.

*n*BMA during the early stages of polymerization, provided that the feed mole fraction of MMA is greater than about 0.4.

As a comparison, in a separate set of experiments, the reactivity ratios of the monomers were determined from copolymers produced by solution polymerization. Table V shows the recipe used for these experiments. Solution volumes were about 25 mL, in which the molar content of monomers was kept constant and the amount of initiator, with respect to monomer content, was kept constant. Polymerizations were done at 70°C for times to yield approximately 5% conversion. The maximum conversion obtained was 7.78%. Polymers were precipitated twice with methanol were then dried to constant weight in vacuum.

Figure 8 also shows the fit to eq. (8), which was obtained for NMR composition data obtained for the solution polymerized copolymers. The reactivity ratios for these polymers were $r_1 = 0.868 \pm 0.028$ and $r_2 = 0.931 \pm 0.037$, in reasonably good agreement with the values found for the emulsion copolymers. Table VI compares the reactivity ratios determined in the present work with values reported in the literature. Clearly there is disagreement between reactivity ratios determined in this study and some of the values reported in the literature. However, it is notable that the determined reactivity ratios are consistent with the published data presented, in that $r_1 < r_2$ and $r_1 r_2 \approx 1$. This is as expected, according to the Q–e scheme of reactivity prediction.[39] Due to similar polarities of the monomers, the reactivities should be close to unity for both monomers by that prediction. Considering that the reactivities for emulsion polymerization yield copolymer compositions that are within 4% of the ideal values, and other reported reactivities yield $r_1 r_2 \approx 1$, it seems reasonable to conclude that the molar copolymer composition is nearly equal to the molar feed composition.

Glass Transition Temperature

Figure 10 shows the glass transitions of the copolymers produced from Table IV. The DSC measurements showed single, narrow transitions, confirming the randomness of the copolymers. The data are observed to be linear with copolymer mass composition and, therefore, they noticeably deviate from Fox's prediction,[20] described by

$$\frac{1}{T_g} = \frac{w_1}{T_{g1}} + \frac{w_2}{T_{g2}} \tag{10}$$

where w_1 and w_2 are the weight fractions of each monomer in the copolymer and T_{g1} and T_{g2} are the absolute glass transition temperatures of the respective homopolymers. Other models have been proposed that attempt to predict glass transition according to either thermal expansion contributions of the constituents in the glassy and rubber phases,[40] or by the AA, BB, AB–BA diad contributions to the transition temperature.[41–43] The latter models depend on knowledge of the AB–BA contribution to the glass transition, T_{gAB}, which is usually considered an adjustable parameter. In general, most of these models yield more pronounced curves than does the Fox relation. Gordon and Taylor,[44] proposed the following

$$T_g = \frac{w_1 T_{g1} + k(1 - w_1) T_{g2}}{w_1 + k(1 - w_1)} \tag{11}$$

where k is a constant for a given copolymer system, usually described as a ratio of thermal expansion coefficients between the rubber and glass phases for the respective homopolymers, $(\alpha_{rb} - \alpha_{gb})/(\alpha_{ra} - \alpha_{ga})$, and the remaining parameters are as defined previously for the Fox equation. For $k = 1$, eq. (11) can be reduced to the following linear form.

$$T_g = w_1 T_{g1} + w_2 T_{g2} \tag{12}$$

The parameter k for the MMA/*n*BMA monomer pair was determined, by the nonlinear regression[45]

Table V Solution Polymerization Recipe Used for Reactivity Ratio Determination

Ingredient	Quantity
Monomer	0.125 (mol/L Solution)
Benzoyl Peroxide	0.0625 (g/mol Monomer)
Toluene	Variable

Table VI Emulsion Polymerization Recipe Used for Kinetic Studies

r_1	r_2	Media
0.758 ± 0.029	0.846 ± 0.044	Emulsion
0.868 ± 0.028	0.931 ± 0.037	Solution
0.79 ± 0.03	1.27 ± 0.05	Solution[a]
0.520 ± 0.070	2.110 ± 0.080	N.A.[b]
0.991	1.007	$Q - e$

[a] Polymerized in bulk and benzene to 5% conversion at 60°C with AIBN initiator.[63]
[b] Method unknown.[46]

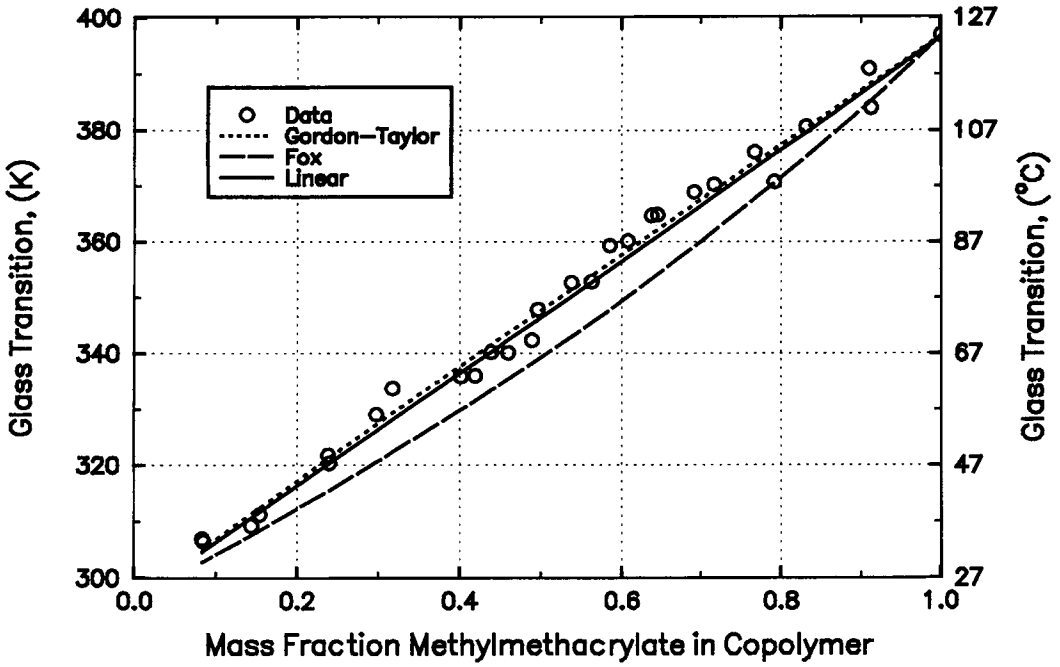

Figure 10 Comparison of experimental T_gs of MMA/nBMA high molecular weight copolymers with various predictions. (– –) Fox, (· · ·) Gordon–Taylor, and (——) linear.

of eq. (11), to be 0.95 ± 0.15. The regression yields values for T_{g1} and T_{g2} of 123.57 ± 3.46°C and 23.28 ± 4.04°C, respectively, which is in excellent agreement with the measured values. Equation (11) yields T_g values within ±2.74°C of the observed values. By comparison, eq. (12) yields T_g values that are within ±2.70°C of the observed values. Considering this insignificant discrepancy between values predicted by eqs. (11) and (12), combined with experimental error, it seems reasonable to assume $k \approx 1$ and to represent the T_g of MMA/nBMA copolymers according to eq. (12).

Chain Transfer

The chain transfer constant for the each of the chosen materials was determined according to well-known chain transfer theory,[32] which states

$$\left(\frac{1}{\overline{X_N}}\right) = \left(\frac{1}{\overline{X_N}}\right)_0 + C_s \frac{[S]}{[M]} \tag{13}$$

where $\overline{X_N}$ and $\overline{X_{N0}}$ are the degrees of polymerization with and without chain transfer, respectively, C_s is the chain transfer constant, and $[S]/[M]$ is the molar ratio of chain transfer agent to monomer. Equation (13) is valid over the entire range of polymerization, as long as the molar ratio $[S]/[M]$ is known. In practice, the conversion of the chain transfer agent is difficult to follow. Therefore, overall conversion of the system is kept low, which allows the initial value of $[S]/[M]$ to be used in eq. (13). In this study, C_s was determined in this manner with conversion based on monomer kept to less than 10%.

Literature information discussing effective chain transfer agents is sparse for MMA and is nonexistent for nBMA. Many tabulated transfer agents

Table VII Physical Properties of Chain Transfer Agents Studied

Material	Formula	FW	ρ, (g/cm^3)	b.p. (°C)
t-Dodecylmercaptan	$C_{12}H_{25}SH$	202.40	0.859	227–248
n-butyl-3-Mercaptopropionate	$HS(CH_2)_2CO_2C_4H_9$	162.25	1.01	101 (12 mm)
iso-Octyl-3-Mercaptopropionate	$HS(CH_2)_2CO_2C_8H_{17}$	218.36	0.963	110 (1 mm)
Thiophenol	C_6H_5SH	110.18	1.073	169

Table VIII Solution Polymerization Recipe for Chain Transfer Constant Determination

Ingredient	Quantity (g)
Monomer	25.00
Toluene	25.00
Benzoyl Peroxide	0.125
Transfer Agent	0.1, 0.2, 0.4, 0.8[a]

[a] Quantity is molar ratio $[S]/[M]$ based on monomer.

have low transfer constants, C_s, many less than 0.01, indicating limited effectiveness.[46] Still others are too effective and yield oligomers of only a few repeat units in length when used.[47] The transfer agents studied here were chosen for their reported effectiveness for molecular weight control in solution or bulk polymerizations of MMA and other monomers. Table VII lists the physical properties of the chain transfer agents studied.

Solution polymerization was used initially to determine the effectiveness of each transfer agent, since this method requires substantially less setup and presumably yields results in a relatively short time that are comparable to emulsion polymerization.[32] Table VIII shows the recipe used for these experiments. Polymerizations were conducted at 70°C with slight agitation under a blanket of nitrogen. The polymer was precipitated with methanol, was washed twice, and was then dried to constant weight in vacuum at 70°C.

Figures 11 and 12 show the results of chain transfer constant determinations of each transfer agent for MMA and *n*BMA, respectively. Table IX lists the results along with comparisons to literature values. The determined values are in fair agreement with the literature values, with the exception of values reported by Sorokina et al.[65] for *t*-DDM in MMA and by the *Polymer Handbook* for THP in MMA. Sorokina et al.[65] noted that the effectiveness of *t*-DDM decreased rapidly with conversion. The reason for this was unclear.

The transfer agent *i*-OMP was chosen as the preferred transfer agent, based on the previous results. This material showed good effectiveness for MMA and reasonable effectiveness for *n*BMA. Of the remaining transfer agents, thiophenol had the greatest efficiency. Since $C_s > 1$ for thiophenol, it would be completely consumed before total conversion of monomer, at which point the molecular weight would begin to grow. To avoid this would require the incremental addition of the transfer agent over the course of the reaction to ensure molecular weight control. This was undesirable. Furthermore, thio-

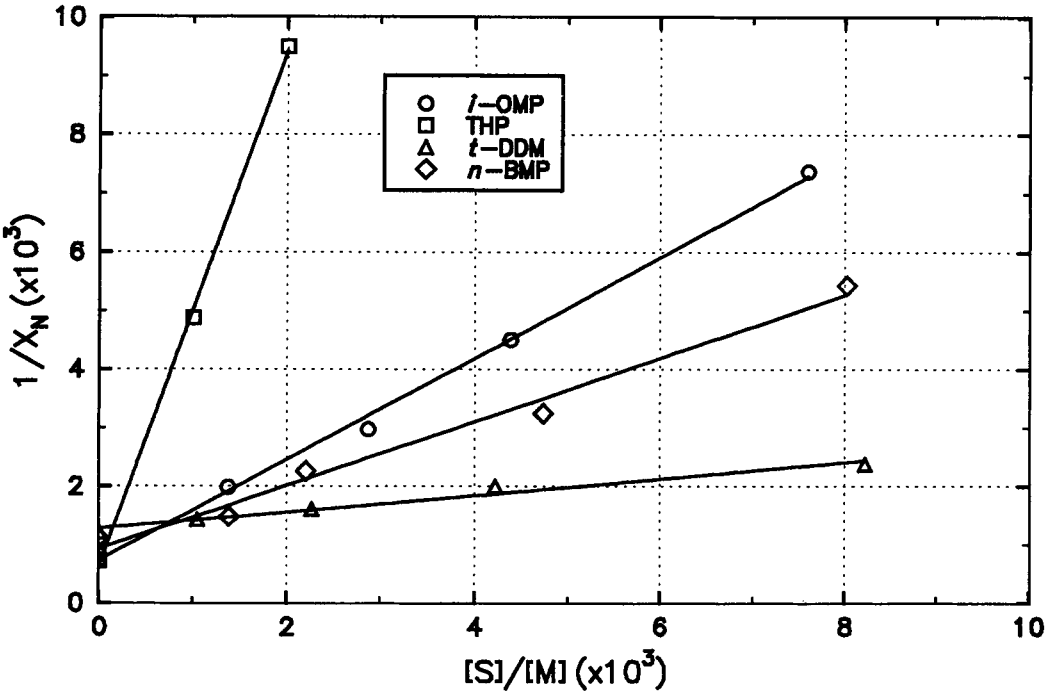

Figure 11 Effectiveness of various chain transfer agents on molecular weight control of methylmethacrylate. Solution polymerized to low conversion in toluene at 70°C.

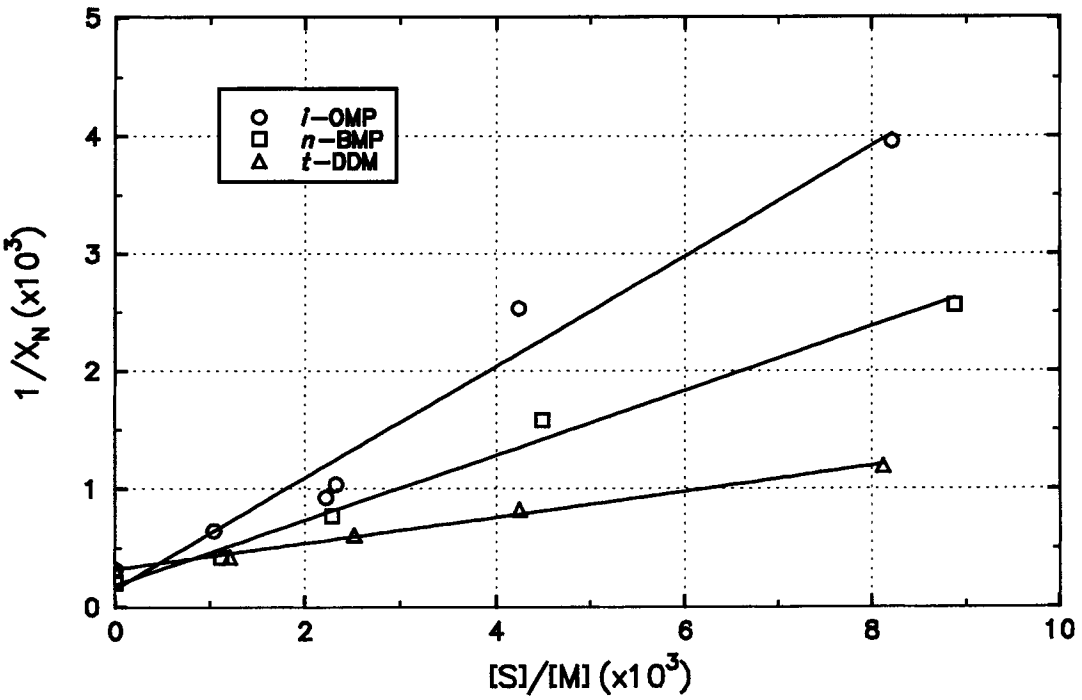

Figure 12 Effectiveness of various chain transfer agents on molecular weight control of *n*-butylmethacrylate. Solution polymerized to low conversion in toluene at 70°C.

phenol is highly toxic and requires special handling precautions. The remaining transfer agents were less effective, yielding $C_s < 0.6$ for MMA. In contrast to thiophenol, these materials would not be wholly consumed during the polymerization, but would require greater starting concentrations to achieve similar molecular weights. *i*-OMP is also preferred because it has no noticeable odor. This feature is a benefit because the polymer with residual transfer agent is to be spray dried.

Table IX Summary of Chain Transfer Constants Determined for MMA and *n*BMA by Solution Polymerization

Monomer	Transfer Agent	C_s	Reported
MMA	*t*-DDM	0.112 ± 0.014	0.13,[a] 0.62[b]
	i-OMP	0.864 ± 0.021	0.54[a]
	n-BMP	0.543 ± 0.038	0.68[a]
	THP	4.396 ± 0.130	2.8,[c] 4.28,[d] 4.7[e]
*n*BMA	*t*-DDM	0.110 ± 0.005	N.A.
	i-OMP	0.472 ± 0.042	N.A.
	n-BMP	0.275 ± 0.016	N.A.

[a] Solution polymerized to high conversion in toluene at 70°C with AIBN initiator.[64]
[b] Bulk polymerized at 60°C with lauryl peroxide initiator.[65]
[c] Solution polymerized in toluene at 60°C with AIBN initiator.[46]
[d] Spontaneously polymerized in benzene 130°C.[66]
[e] Bulk polymerized at 45°C with AIBN initiator.[67]

The chain transfer experiments were repeated for *i*-OMP with both monomers in emulsion polymerization using the standard recipe at 50°C. Monomer conversion was followed gravimetrically and chain transfer constants were determined from polymer samples obtained at about 5% conversion. The observed rates of polymerization were unaffected by the presence of *i*-OMP in accordance with observations made by Smith.[48] Furthermore, during polymerizations with MMA, the addition of *i*-OMP reduced or eliminated the "gel effect" because of the lowering of polymer viscosity.

Generally, it has been proposed that C_s should not change from solution to emulsion polymerization, provided that diffusion of the modifier is not limiting.[32] However, this was not the case for the transfer agent studied. Figure 13 shows the transfer constants determined for both MMA and *n*BMA. There is a complete reversal in the effectiveness of the transfer agent and repeated experiments only confirmed this fact. The reason for this is unclear. It is possible this discrepancy may arise from a combination of two factors.

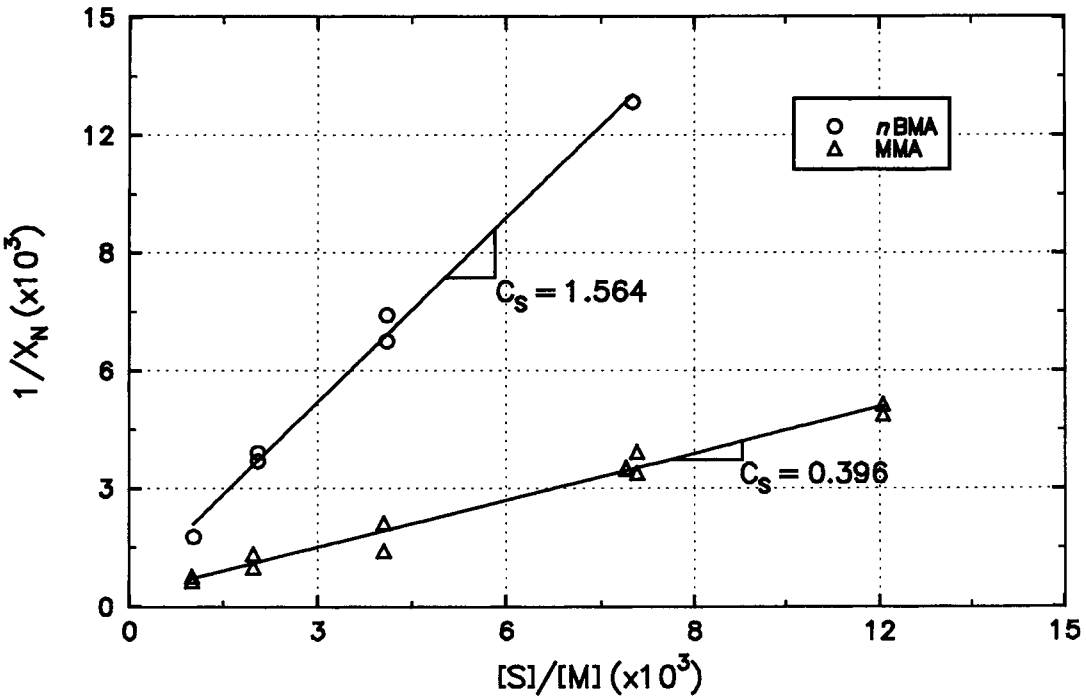

Figure 13 Effectiveness of *i*-OMP as chain transfer agent on emulsion homopolymerization of MMA and *n*BMA at ~5% conversion.

First, the high molecular weight of *i*-OMP may impede diffusion through the continuous aqueous phase to the locus of polymerization. Smith[48] showed a dependence of transfer agent molecular weight on its effectiveness in the emulsion polymerization of styrene. For normal mercaptans, the transfer constant, C_s, was shown to decrease dramatically as the number of carbon atoms exceeded ten. Kolthoff and Harris,[49] studying the effects of molecular structure, showed similar results for the emulsion copolymerization of butadiene–styrene. Kolthoff and Harris,[49] as well as Uraneck and Burleigh,[50] have indicated a dependence of transfer agent effectiveness on the mode and rate of agitation of the emulsion during polymerization. In the present work, however, stirring was found to have no influence on the effectiveness of *i*-OMP.

Second, the method of particle nucleation may play a role in the effectiveness of the transfer agent. It has been shown that monomer solubility determines the locus of particle nucleation in emulsion polymerization.[51,52] Slightly soluble monomers, such as MMA (1.5% wt, 25–50°C),[53] are observed to form aqueous phase oligomers in the early stages of polymerization and to precipitate into surfactant stabilized micelles, subsequently forming monomer swollen polymer particles in later stages of polymerization. In contrast, insoluble monomers, such as *n*BMA (0.078% wt, 50°C),[51] are observed to follow the more accepted emulsion polymerization mechanism, as defined by Smith–Ewart. If these observations are indeed true, then it is expected that the transfer agent *i*-OMP, which is only sparingly soluble in water, would have little effect on the molecular weight of PMMA in the early stages of the polymerization. However, following particle nucleation, it would be expected that chain transfer would continue unhindered. Particle nucleation is generally considered to be complete in the region of 10–30% conversion, corresponding to the beginning of the constant rate period of the conversion curve.[19,32,54,55] In the present work, constant polymerization rates were fully developed at about 10–15% conversion for both MMA and *n*BMA. Figure 14 shows the transfer constants obtained for both monomers from polymer samples obtained at 20% conversion. The transfer constant, obtained for the MMA system, is seen to increase, suggesting that polymer growth has transferred to a locus richer in transfer agent. Furthermore, the transfer constant for *n*BMA is seen to decrease. This is as expected, since $C_s > 1$ at 5% conversion results in rapid depletion of the transfer agent before complete monomer conversion.

The effectiveness of *i*-OMP was studied for the copolymerization of MMA/*n*BMA and was compared to the overall transfer constant predicted by

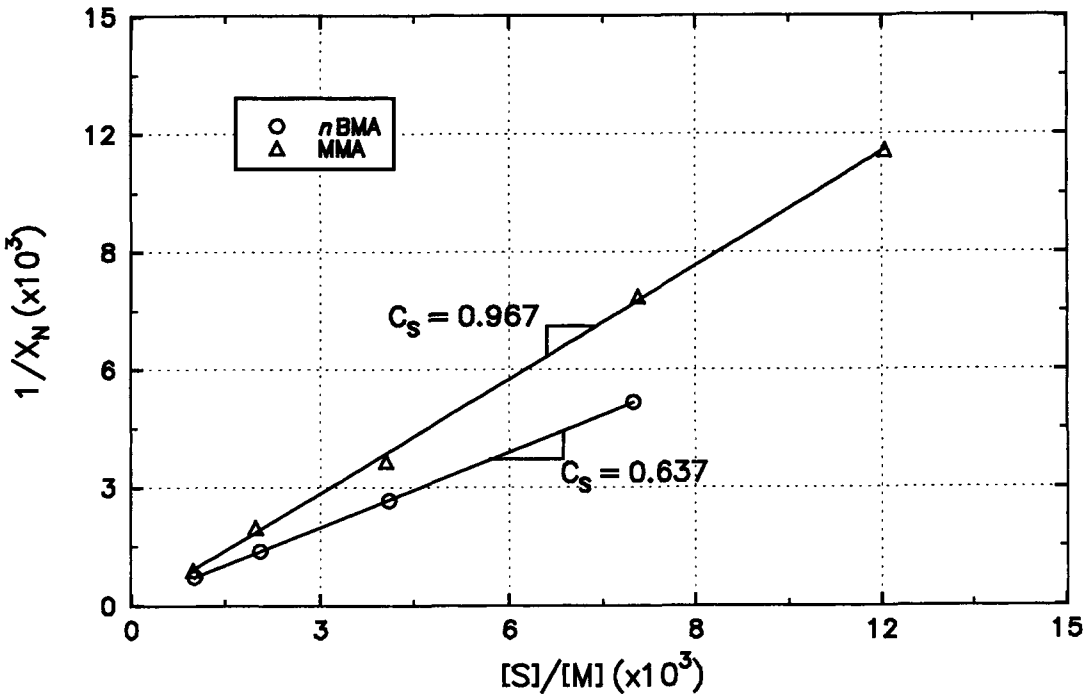

Figure 14 Effectiveness of *i*-OMP as chain transfer agent on emulsion homopolymerization of MMA and *n*BMA at ~20% conversion.

kinetic theory. Smith[56] showed that the overall transfer constant, C, derived from the consumption of both transfer agent and comonomers, could be expressed as follows

$$\frac{d\ln[S]}{d\ln(x_1 + x_2)} = \frac{C_{s1}r_1x_1 + C_{s2}r_2x_2}{r_1x_1^2 + 2x_1x_2 + r_2x_2^2} = C \quad (14)$$

where

$$C_{s1} = \frac{k_{tr1}}{k_{11}}; \quad C_{s2} = \frac{k_{tr2}}{k_{22}} \quad (15)$$

where the homopolymerization chain transfer constants, x_1 and x_2, are the mole fractions of the respective monomers in the overall system, r_1 and r_2 are the reactivity ratios as defined previously, and C is the overall chain transfer constant. Smith verified eq. (14) in the emulsion polymerization of styrene–methylmethacrylate, using reactivity ratios determined in solution by arguing r_1 and r_2 should not be different between emulsion and solution polymerization, because the consumption of monomer in emulsion was not diffusion controlled.

To avoid the difficulties of following transfer agent conversion in order to evaluate the overall transfer constant, C, from eq. (14), it was convenient to determine C from an analogue to eq. (13). The derivation of this analogue is similar to that of eq. (13) and assumes the rate of copolymerization is not diffusion controlled.[38,57] The kinetic chain length, $\bar{\nu}$, is defined as

$$\bar{\nu} = \frac{R_p}{R_i} \quad (16)$$

where R_p is the rate of copolymerization and R_i is the rate of radical initiation. From the propagation steps, assuming equivalent cross propagation, the rate of copolymerization, R_p, is

$$R_p = \frac{k_{11}}{r_1}\frac{[M_1^\cdot]}{[M_1]}(r_1[M_1]^2 + 2[M_1][M_2] + r_2[M_2]^2) \quad (17)$$

At steady state, the rate of radical initiation is equal to the rate of radical termination, R_t. Assuming persulfate initiation, this is defined as

$$R_t = R_i = 2k_d[I] = 2[M_1^\cdot]^2\left(k_{t_{11}} + \frac{k_{t_{22}}k_{12}^2}{k_{12}^2}\frac{[M_2]^2}{[M_1]^2} + \frac{k_{t_{12}}k_{12}}{k_{21}}\frac{[M_2]}{[M_1]}\right) + [SH][M_1^\cdot]\left(k_{tr_1} + \frac{k_{tr_2}k_{12}}{k_{21}}\frac{[M_2]}{[M_1]}\right) \quad (18)$$

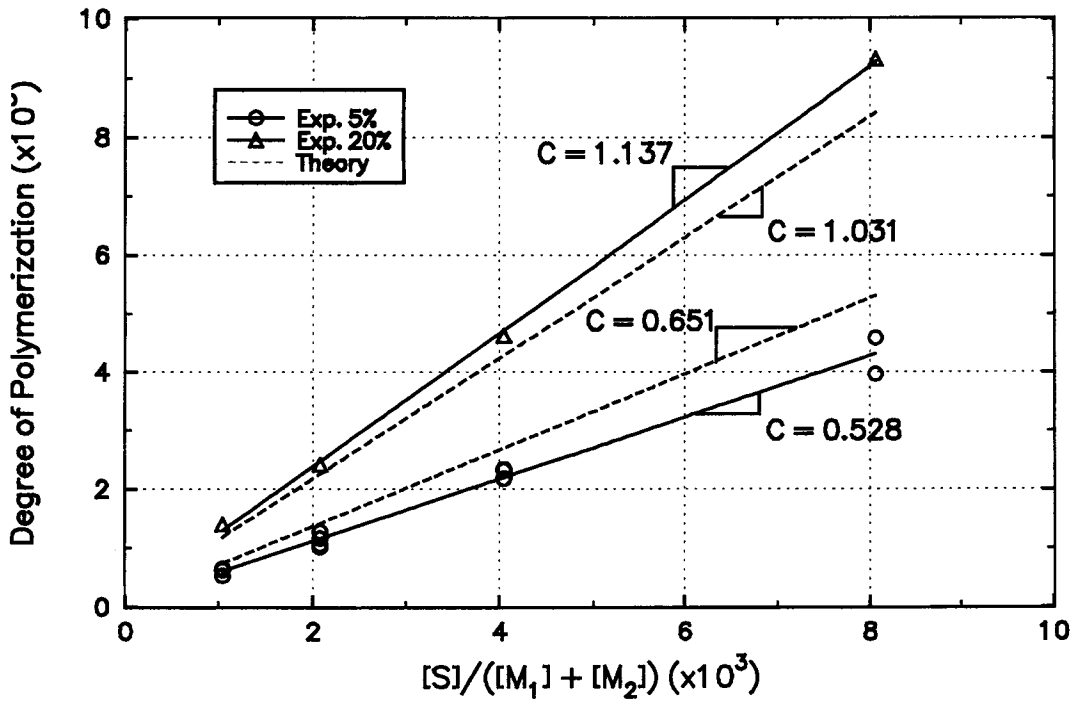

Figure 15 Comparison of effective chain transfer constant, C, for i-OMP to theory for emulsion copolymerization of MMA/nBMA. Molar feed ratio 75/25 (MMA/nBMA).

where the second term of the third equality is due to termination by chain transfer. Substitution of eqs. (17) and (18) into eq. (16), combined with the definitions presented by Smith,[56] yields the analogous form of eq. (13), which is

$$\left(\frac{1}{\bar{\nu}}\right) = \left(\frac{1}{\bar{\nu}}\right)_0 + \left(\frac{C_{s_1} r_1 x_1 + C_{s_2} r_2 x_2}{r_1 x_1^2 + 2x_1 x_2 + r_2 x_2^2}\right) \frac{[SH]}{[M_1] + [M_2]} \tag{19}$$

Equation (19) is subject to the same constraints in overall conversion as prescribed for eq. (13).

Copolymerization with chain transfer was conducted, as before, for the emulsion homopolymerization of the respective monomers, except that the transfer agent molar content was based on the total monomer molar content, according to the last term on the right side of eq. (19). Figure 15 compares the effective transfer constant determined for a copolymer that had a molar feed ratio of 75/25 MMA/nBMA to the value predicted by eq. (19), using $r_1 = 0.758$, $C_{s1} = 0.396$, $r_2 = 0.846$, $C_{s2} = 1.564$, for 5% conversion, and $r_1 = 0.758$, $C_{s1} = 0.967$, $r_2 = 0.846$, $C_{s2} = 0.637$, at 20% conversion, determined for emulsion polymerization in this work. Due to the results presented above, which showed a dependence of the transfer constant on conversion, the effective transfer constant for copolymerization was determined at 5% and 20% conversion. The experimental values determined are within 20% of the predicted values for both levels of conversion. This agreement is good, considering the complexity of the system and the uncertainty of the determined constants.

Molecular Weight Effects

It is well known that polymer viscosity is a strong function of molecular weight[38] according to the relation

$$\eta = KM_w^a \tag{20}$$

where K is a function of temperature and the exponent a has a value 3.4 for nearly all polymers, provided that the molecular weight is above some critical value, W_c. Polymer melt flow properties are inversely proportional to viscosity and, in the limit of Newtonian flow, melt flow can be related to molecular weight using eq. (20). Combining this result with eq. (13) leads to the following expression:

$$M.I. = \left(\frac{1}{M_{w_0}}\right)^a \left(1 + M_{w_0} K' \frac{[SH]}{[M]}\right)^a \tag{21}$$

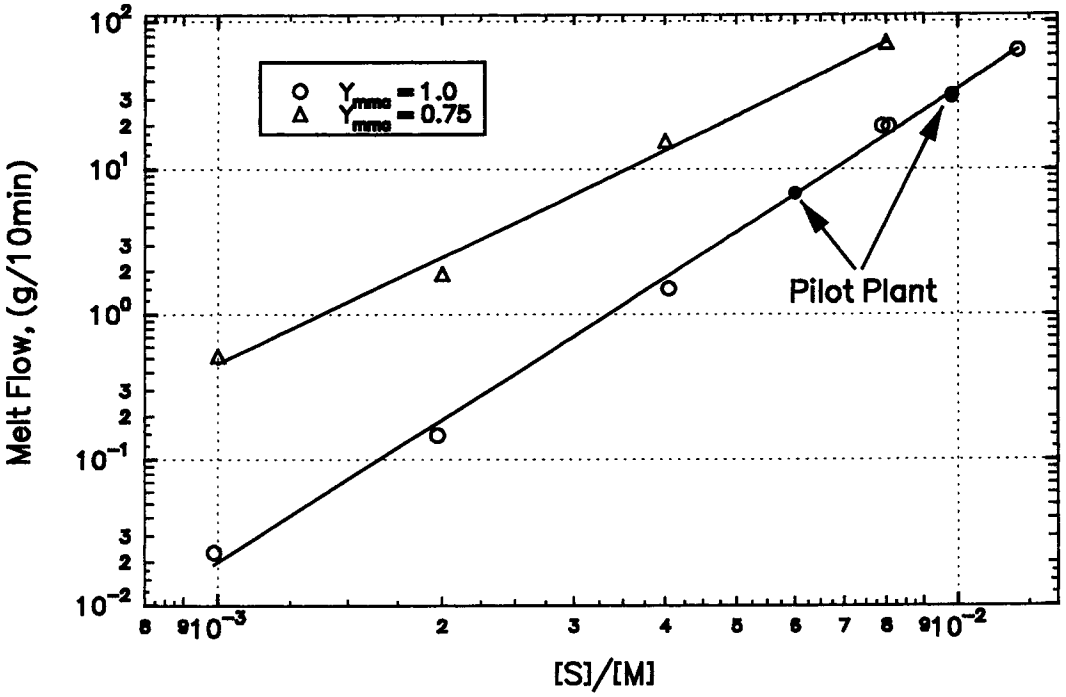

Figure 16 Effect of chain transfer on melt flow index of PMMA and P(MMA-*co*-*n*BMA) (75/25 mole fraction in feed), measured at 200°C and 0.52 MPa (75 psi).

where *M.I.* is the melt flow index, M_{W0} is the molecular weight with no chain transfer, and K' is a new constant, which is a function the chain transfer constant, C_s. Since the term $M_{W0}K' \gg 1$, eq. (21) can be reduced to a form similar to eq. (20), as follows

$$M.I. = K'\left(\frac{[S]}{[M]}\right)^a \tag{22}$$

Figure 16 shows the results of melt flow index measurements done on PMMA and P(MMA-*co*-*n*BMA) polymers, plotted according to eq. (22). The fits are good and yield the following expressions:

$$M.I._{\text{PMMA}} = 100.7 \times 10^6\left(\frac{[S]}{[M]}\right)^{3.2}$$

$$M.I._{CO_{75/25}} = 941.4 \times 10^3\left(\frac{[S]}{[M]}\right)^{2.4} \tag{23}$$

These expressions provide a convenient means of obtaining polymers with specified melt flow values, based on feed conditions. Equation (23) has been used with good success during scale-up of PMMA to a 20 liter pilot plant and in laboratory experiments with MMA/*n*BMA copolymers.

Changes in polymer molecular weight are observed to affect polymer glass transition[58] as follows

$$T_g = T_{g\infty} - \frac{k_{T_g}}{M_N} \tag{24}$$

where $T_{g\infty}$ is the glass transition for infinite molecular weight, k_{T_g} is a constant, and M_N is the number average molecular weight. Using eq. (13), eq. (24) can be expressed conveniently in terms of the quantity $[S]/[M]$. Figure 17 shows the results of glass transition for PMMA and P(MMA-*co*-*n*BMA) polymers, plotted according to a modified eq. (24). The equation fits are linear and are expressed as

$$T_{g\text{PMMA}} = 397.8 - 2429.6\left(\frac{[S]}{[M]}\right)$$

$$T_{g_{\text{co}75/25}} = 363.4 - 1359.4\left(\frac{[S]}{[M]}\right) \tag{25}$$

The apparent effect of molecular weight on the glass transition of PMMA is pronounced. The glass transition temperature of a 30 g/10 min melt flow PMMA ($[S]/[M] = 9.8 \times 10^{-3}$) is about 100°C, nearly a 20°C drop in T_g, relative to the high molecular weight limit. The T_g depression is not as pro-

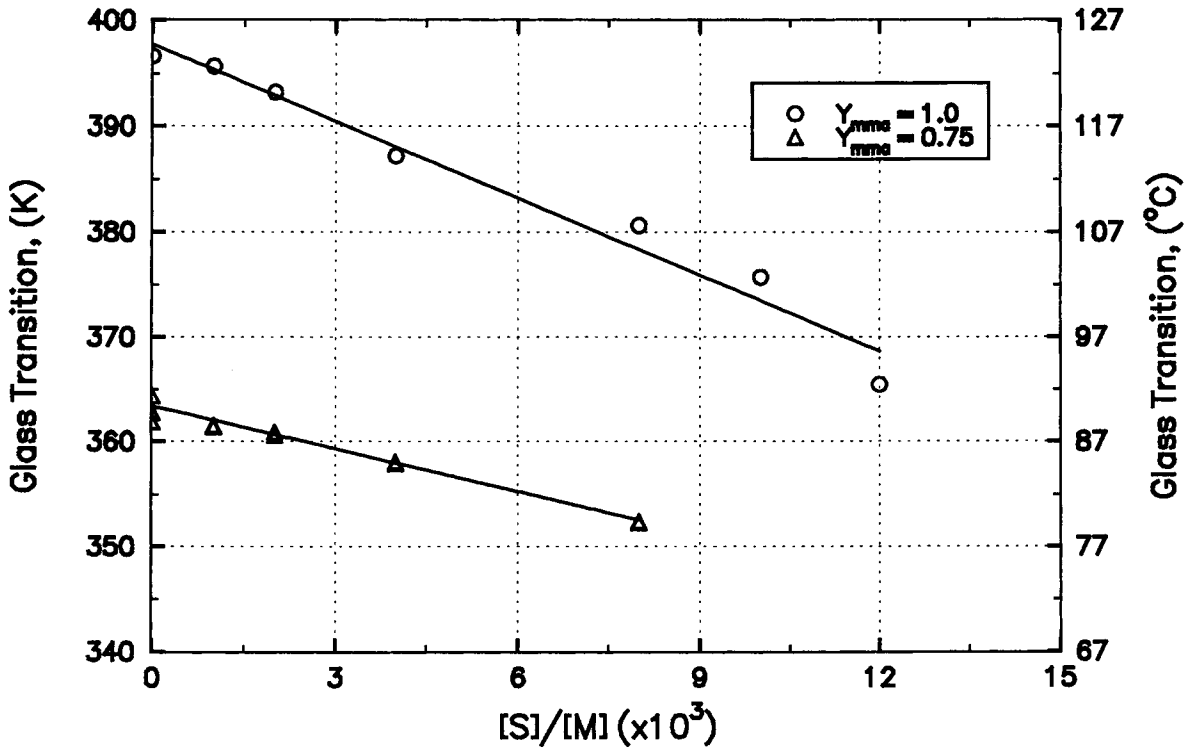

Figure 17 Effect of chain transfer on the glass transition of PMMA and P(MMA-*co*-*n*BMA) (75/25 mole fraction in feed).

nounced for the copolymer shown. However, since polymer melt flow and glass transition temperature are important quantities with respect to powder coating conditions and SLS processing conditions, the ability to predict these quantities for tailored MMA/*n*BMA copolymers, using the above equations, is an important tool.

Binder Performance

Figure 18 shows 3-point bend green strengths of 3 in. × 1 in. × $\frac{1}{4}$ in. test specimens made from PMMA-coated (20% vol, 8.5% wt) silicon carbide using SLS.[59] The data show the development of bend strength with increasing laser power density, A_N, a parameter characteristic of SLS that is derived from scanning and part geometries.[60] As indicated by Figure 18, green strengths near 200 psi are obtainable, yielding objects that can be easily handled.

Preliminary work with an 80/20 MMA/*n*BMA molar feed ratio copolymer binder indicates similar strength results to the PMMA binder discussed above. Figure 19 shows 3-point bend strengths of a series of 80/20 copolymers with varying molecular weights as compared to strengths of a PMMA binder and two commercial latex polymers. The commercial latex polymers were UCAR-430, a styrene–methylmethacrylate–butylacrylate–methacrylic acid copolymer supplied by Union Carbide Corporation, and CR763, a styrene–ethylacrylate copolymer supplied by B.F. Goodrich, Inc. UCAR-430 was used in early studies at The University of Texas.[1] CR763 is a binder currently being evaluated by DTM Corporation. The bulk polymer specimens were 4 in. × 1 in. × $\frac{1}{8}$ in. samples cut from a compression molded sheet. The composite specimens were produced from a mixture of spray dried polymer powder (22.4% vol, 11.2% wt) with a spherical soda-lime glass (A-3000 Potters Industries, Inc., D_p = 24.0 μm). The mixture was placed in an aluminum die containing six specimen cavities 3 in. × 1 in. × $\frac{1}{4}$ in. and was baked at 175°C for $\frac{1}{2}$ h.

Figure 19 clearly shows the influence of molecular weight on the strength properties of both the bulk polymers and the composite materials. As the molecular weight decreases, the bulk strength of the polymer remains essentially constant to a certain point, then drops rapidly with further decreases in molecular weight. In contrast, the strength of the composite materials are seen to increase dramatically to a plateau value with decreases in molecular

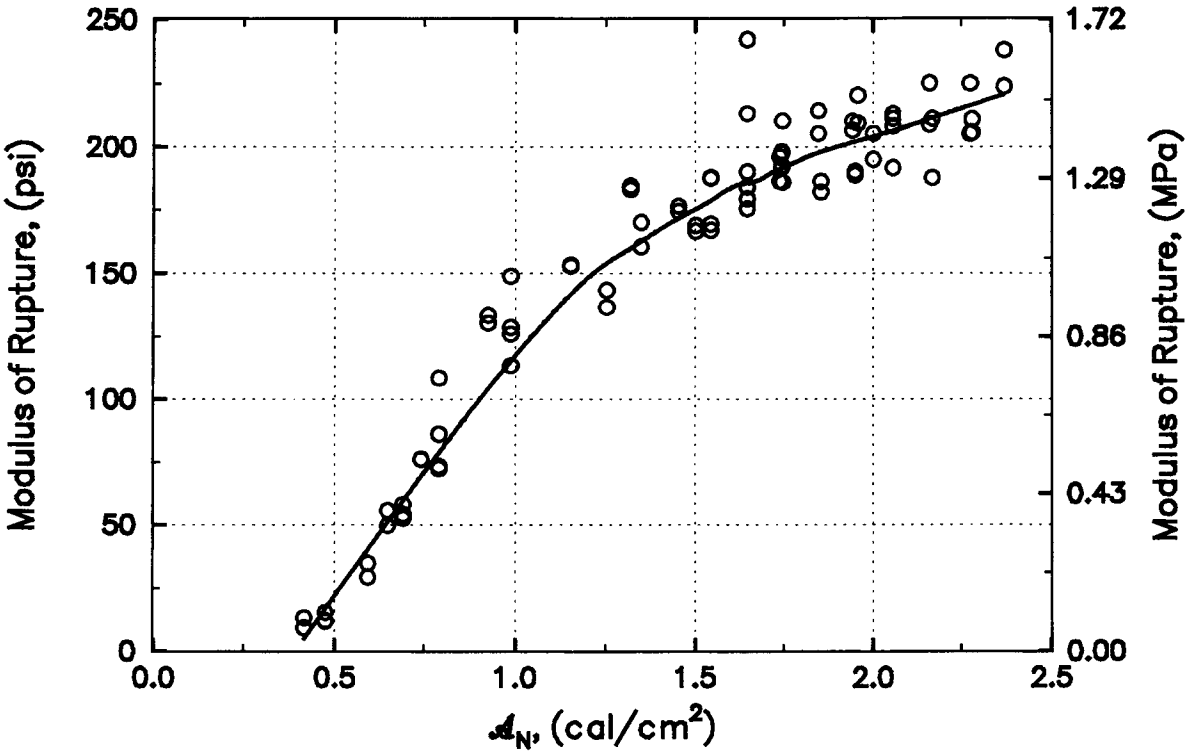

Figure 18 Strength development of selective laser sintered PMMA coated silicon carbide with laser power scan density, with 20% vol (8.5% wt) polymer content.

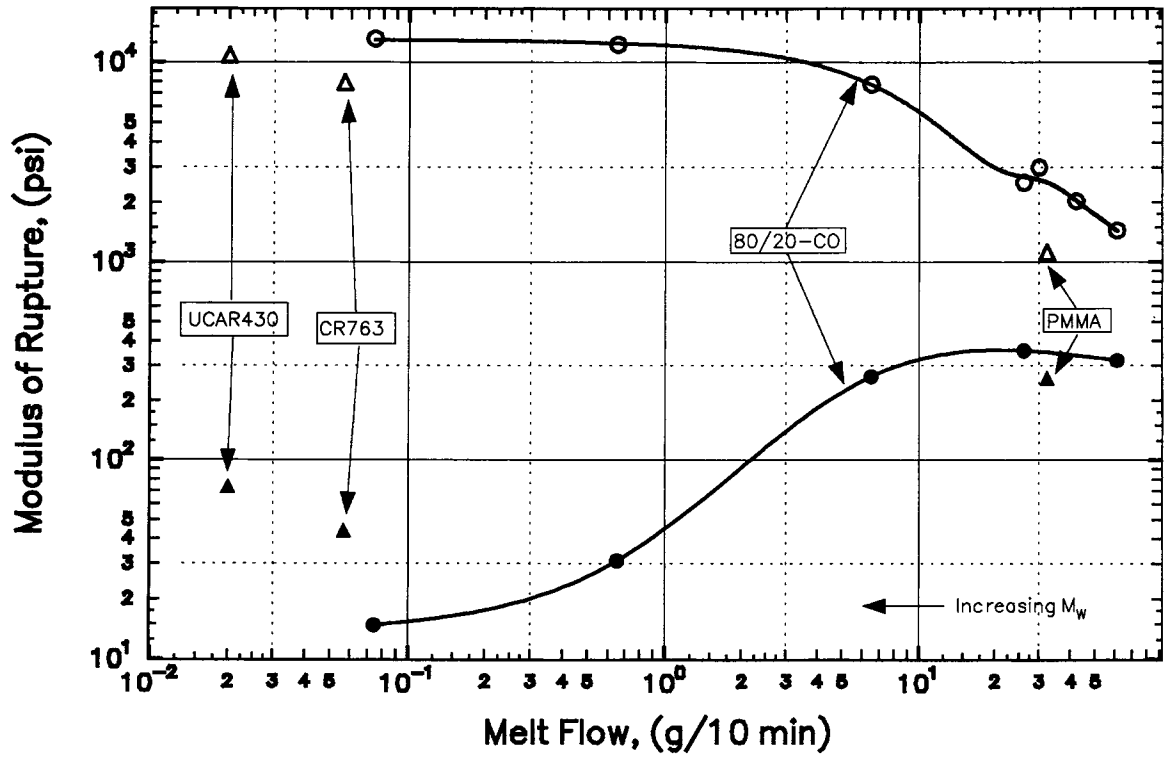

Figure 19 Open symbols: bulk polymer strengths with molecular weight. Closed symbols: Polymer/glass composite strengths with molecular weight. Polymer content 22.4% vol (11.2% wt).

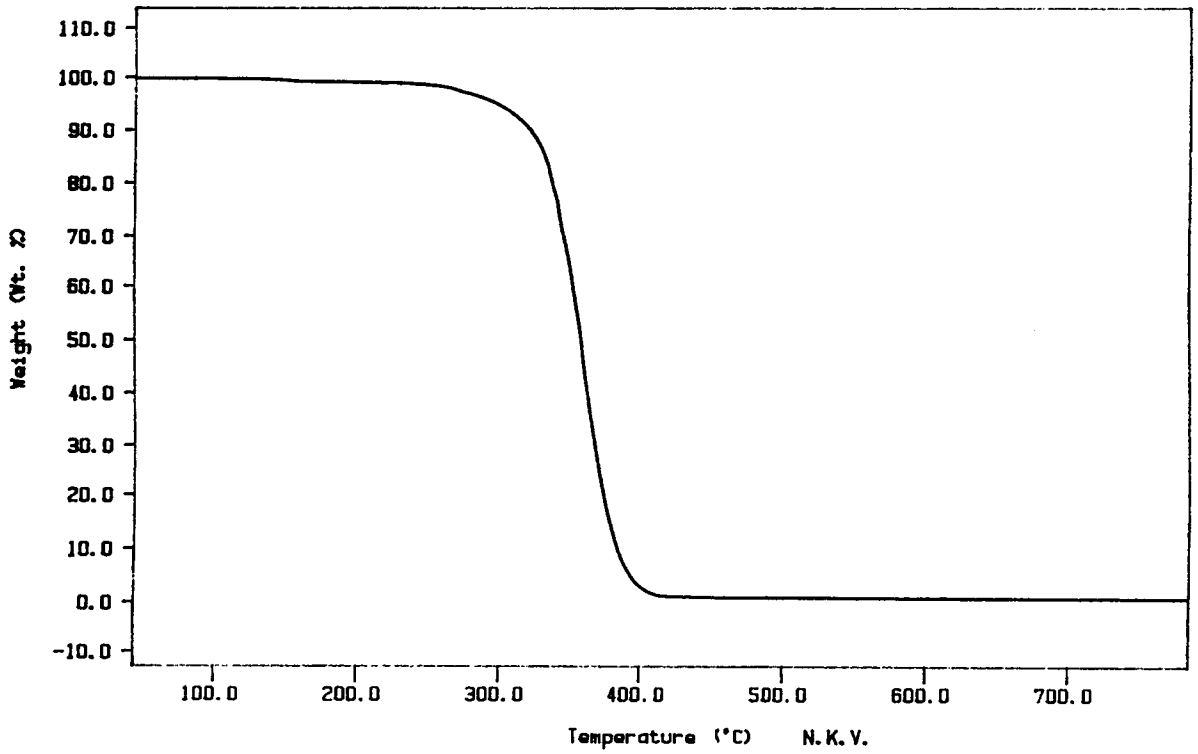

Figure 20 Thermal gravimetric analysis trace of an 80/20 MMA/*n*BMA molar feed copolymer having melt flow index of 6.5 g/10 min. Heating rate 10.0°C/min, N_2 atmosphere.

weight. This result emphasizes the role of polymer molecular weight in wetting of powder substrates and promoting the development of good polymer to solid adhesion. Figure 19 provides the impetus for the copolymer research presented here.

Thermal decomposition analysis of the polymer systems developed here indicate the polymer to decompose fully in a nonoxidizing environment. Figure 20 shows a thermal gravimetric analysis (TGA) trace of an 80/20 MMA/*n*BMA copolymer, having a melt flow of 6.5 g/10 min at 200°C and 0.52 MPa (75 psi). The polymer sample was prepared by drying a portion of latex in air at 75°C to constant weight, producing fine granules. The analysis indicates that at about 450°C, approximately 0.49 wt % of the pure polymer system remains. This amount of residue is not significant considering that the polymer binder comprises less than 10 wt % of a typical material system used for SLS. However, since emulsifier and initiator are still present in the dried polymer sample, the decomposition products of these materials must be considered as part of the polymer ash. TGA analysis of sodium dodecyl sulfate and potassium persulfate were conducted at conditions identical to that of Figure 20. At 450°C SDS shows approximately 25 wt % residue and, similarly, the initiator shows about 55 wt % residue. A mass balance of the system indicates the polymer sample ash to be mostly emulsifier and initiator decomposition byproducts.

CONCLUSIONS

A method of producing low molecular weight poly(methylmethacrylate) and poly(methylmethacrylate-*co*-*n*-butylmethacrylate) emulsion polymers has been developed. The polymers developed have been characterized kinetically with respect to reaction rates, reactivity ratios of the respective monomers, and the influence of chain transfer. Furthermore, the physical properties of the polymers developed have been characterized with respect to molecular weight dependence of chain transfer, and molecular weight dependence on glass transition temperature. The comonomers studied yield a nearly ideal copolymer system of random composition. The glass transition of P(MMA-*co*-*n*BMA) copolymers are linearly related to the homopolymer glass transitions and comonomer mass fraction content. The ability to obtain polymers with predictable melt flows and glass transition temperatures has been useful in the development and evaluation of

polymer-coated materials used in selective laser sintering.

The polymers developed here have been shown to be effective fugitive binders for the manufacture of SLS green parts from a variety ceramic and metal materials. Acceptably strong green shapes, using low binder volume contents, have been produced from several ceramic systems, including glass,[6,61] alumina,[8] silica–zircon,[8] and silicon carbide.[59] Metal systems, including iron and copper,[62] are also showing similar success with these binders. Furthermore, during subsequent postfiring of these metal systems, the binder has been shown to be fully decomposing, leaving insignificant carbon residue.

Partial support for this research by the Advanced Research Projects Agency/ONR, Grant #0001492J1394, is gratefully acknowledged. DTM Corporation made available the SLS Model 125 workstation for these studies. Appreciation is given to Mike Durham, of the Austin Service Bureau, for his cooperation in obtaining experiment time on the workstation.

REFERENCES

1. D. L. Bourell, J. J. Beaman, H. L. Marcus, and J. W. Barlow, *Solid Freeform Fabrication Symposium Proceedings,* **1,** 1 (1990).
2. S. Ashley, *Mech. Eng.,* **113**(4), 34 (1991).
3. C. R. Deckard, M.S. Thesis, Dept. of Mech. Eng., The University of Texas at Austin, 1986.
4. C. R. Deckard, Ph.D. Dissertation, Dept. of Mech. Eng., The University of Texas at Austin, 1988.
5. G. Zong, Y. Wu, N. Tran, I. Lee, D. L. Bourell, and H. L. Marcus, *Solid Freeform Fabrication Symposium Proceedings,* **3,** 72 (1992).
6. B. Balasubramanian and J. W. Barlow, *Solid Freeform Fabrication Symposium Proceedings,* **2,** 245 (1991).
7. N. K. Vail and J. W. Barlow, *Solid Freeform Fabrication Symposium Proceedings,* **2,** 195 (1991).
8. N. K. Vail and J. W. Barlow, *Solid Freeform Fabrication Symposium Proceedings,* **3,** 124 (1992).
9. N. K. Vail, Ph.D. Dissertation, to appear.
10. N. K. Vail and J. W. Barlow, *Solid Freeform Fabrication Symposium Proceedings,* **1,** 8 (1990).
11. K. Masters, *Spray Drying Handbook, 4th Ed.,* Wiley, New York, 1985.
12. A. Kondo, *Microcapsule Processing and Technology,* Marcel Dekker, New York, 1979.
13. W. S. Zimmt, *J. Appl. Polym. Sci.,* **1**(3), 323 (1959).
14. J. H. Baxendale, M. G. Evans, and J. K. Kilham, *J. Polym. Sci.,* **1**(6), 466 (1946).
15. S. Lora, G. Palma, L. Busulini, and B. Castilletti, *Eur. Polym. J.,* **10,** 1223 (1974).
16. K. Ito and K. F. O'Driscoll, *J. Polym. Sci. Chem. Ed.,* **17,** 3913 (1979).
17. J. G. Brodnyan, J. A. Cala, T. Konen, and E. L. Kelley, *J. Colloid Sci.,* **18,** 73 (1963).
18. R. T. Conley, *Thermal Stability of Polymers, Vol. 1,* Marcel Dekker, New York, 1970.
19. *Encyclopedia of Polymer Science and Engineering,* Wiley, New York, 1986.
20. T. G. Fox, *Bull. Am. Phys. Soc.,* **1,** 123 (1956).
21. J. S. Reed, *Introduction to the Principles of Ceramic Processing,* Wiley, New York, 1988.
22. F. M. Fowkes, *Proceedings of the International Symposium on Physicochemical Aspects of Polymer Surfaces,* **2,** 583 (1983).
23. S. Ellerstein and R. Ullman, *J. Polym. Sci.,* **55,** 123 (1961).
24. W. V. Smith and R. H. Ewart, *J. Chem. Phys.,* **16,** 592 (1948).
25. M. Hasagawa, K. Arai, and S. Saito, *J. Polym. Sci. Part A Chem. Ed.,* **25,** 3231 (1987).
26. J. L. Gardon, *J. Polym. Sci. Part A-1,* **6,** 2853 (1968).
27. M. A. Schmerling, Ph.D., private communication.
28. J. G. Brodnyan, *J. Colloid Sci.,* **15,** 563 (1960).
29. J. T. Lazor, *J. Appl. Polym. Sci.,* **1,** 11–16 (1959).
30. H. Gerrens, *Z. Electrochem.,* **67,** 741 (1961).
31. M. J. Ballard, D. H. Napper, and R. G. Gilbert, *J. Polym. Sci. Polym. Chem. Ed.,* **22,** 3225 (1984).
32. F. A. Bovey, I. M. Kolthoff, A. I. Medalia, and E. J. Meehan, *Emulsion Polymerization,* Interscience, New York, 1955.
33. M. H. Mackay and H. W. Melville, *Trans. Faraday Soc.,* **45,** 323 (1949).
34. F. A. Bovey, *Nuclear Magnetic Resonance Spectroscopy, 2nd. Ed.,* Academic Press, San Diego, 1988, Chap. 7.
35. C. J. Pouchert, *The Aldrich Library of NMR Spectra, 2nd Ed.,* Aldrich Chemical, Milwaukee, 1983.
36. M. Fineman and S. D. Ross, *J. Polym. Sci.,* **5,** 259 (1950).
37. T. Kelen and F. Tüdõs, *J. Macro. Sci. Chem.,* **A9**(1), 1 (1975).
38. F. W. Billmeyer, *Textbook of Polymer Science, 3rd. Ed.,* Marcel Dekker, New York, 1970.
39. P. Munk, *Introduction to Macromolecular Science,* Wiley, New York, 1989.
40. L. A. Wood, *J. Polym. Sci.,* **28,** 319 (1958).
41. E. L. Madruga, J. San Román, and J. Guzmán, *J. Macro. Sci. Chem.,* **A13**(8), 1089 (1979).
42. K. Tada, F. Takayuki, and J. Furukawa, *J. Polym. Sci. Part A-1,* **4,** 2981 (1966).
43. J. Furukawa, *J. Polym. Sci. Sym. Series #51,* 105 (1975).
44. O. Olabisi, L. M. Robeson, and M. T. Shaw, *Polymer–Polymer Miscibility,* Academic, New York, 1979.
45. E. L. Crow, F. A. Davis, and M. W. Maxfield, *Statistics Manual,* Dover, New York, 1960.
46. J. Brandrup and E. H. Immergut, *Polymer Handbook, 3rd. Ed.,* Wiley, New York, 1989.
47. R. A. Sanayei and K. F. O'Driscoll, *J. Macro. Sci. Chem.,* **A26**(8), 1137 (1989).
48. W. V. Smith, *J. Am. Chem. Soc.,* **68,** 2059 (1946).

49. I. M. Kolthoff and W. E. Harris, *J. Polym. Sci.*, **2**, 49 (1947).
50. C. A. Uraneck and J. E. Burleigh, *J. Appl. Polym. Sci.*, **17**, 2667 (1973).
51. V. I. Eliseeva, S. S. Ivanchev, S. I. Kuchanov, and A. V. Lebedev, *Emulsion Polymerization and Its Applications in Industry*, Consultants Bureau, New York, 1981.
52. J. H. Baxendale, M. G. Evans, and J. K. Kilham, *Trans. Faraday Soc.*, **42**, 668 (1946).
53. D. T. Wasan, M. E. Ginn, and D. O. Shah, *Surfactants in Chemical/Process Engineering*, Marcel Dekker, New York, 1988.
54. P. Rempp, *Polymer Synthesis*, Hüthig and Wepf, Heidelberg, 1986.
55. J. L. Gardon, *J. Polym. Sci. Part A-1*, **6**, 623 (1968).
56. W. V. Smith, *J. Am. Chem. Soc.*, **68**, 2069 (1946).
57. G. Odian, *Principles of Polymerization*, McGraw-Hill, New York, 1981.
58. S. Wu, *Polymer Interface and Adhesion*, Marcel Dekker, New York, 1982.
59. N. K. Vail, J. W. Barlow, and H. L. Marcus, *Solid Freeform Fabrication Symposium Proceedings*, **4**, 204 (1993).
60. J. C. Nelson, Ph.D. Dissertation, Dept. of Chem. Eng., The University of Texas at Austin, 1993.
61. K. A. Bartels, R. H. Crawford, S. Das, S. Guduri, A. C. Bovik, K. R. Diller, and S. J. Aggarwal, *J. Microscopy*, **169**(3), 383 (1992).
62. B. Badrinarayan, J. R. Tobin, J. W. Barlow, J. J. Beaman, and D. L. Bourell, *Solid Freeform Fabrication Symposium Proceedings*, **4**, 204 (1993).
63. J. C. Bevington and D. O. Harris, *J. Polym. Sci. B*, **5**, 799 (1967).
64. I. Segall and M. S. El-Aasser, *#14 in Emulsion Polymers Institute: Graduate Research Progress Reports, No. 35*, Lehigh University, 1991.
65. L. I. Sorokina, T. I. Radbil, G. N. Sorokina, and B. P. Shilarkman, *Plast. Massy*, **9**, 57 (1983).
66. J. Lingnau and G. Meyerhoff, *Polymer*, **24**(11), 1473 (1983).
67. S. C. Barton, R. A. Bird, and K. E. Russell, *Can. J. Chem.*, **41**, 2737 (1963).

Received August 19, 1993
Accepted October 27, 1993